

Cosmological Dependence of Non-resonantly Produced Sterile Neutrinos

Graciela B. Gelmini,^a Philip Lu^a and Volodymyr Takhistov^a

^a*Department of Physics and Astronomy, UCLA,
475 Portola Plaza, Los Angeles, CA 90095, USA*

E-mail: gelmini@physics.ucla.edu, philiplu11@gmail.com,
vtakhist@physics.ucla.edu

Abstract: We discuss how a laboratory detection of a sterile neutrino not only would constitute a fundamental discovery of a new particle, but could also provide an indication of the evolution of the Universe before Big-Bang Nucleosynthesis (BBN), a fundamental discovery in cosmology. These “visible” sterile neutrinos could be detected in experiments such as KATRIN/TRISTAN and HUNTER in the keV mass range and PTOLEMY, KATRIN and reactor neutrino experiments in the eV mass range. Standard assumptions are usually made to compute the relic abundance and momentum distribution of particles produced before the temperature of the Universe was 5 MeV, an epoch from which there are no observed remnants thus far. However, non-standard pre-BBN cosmologies based on other assumptions that are equally in agreement with all existing data can arise in some theoretical models. We revisit the production of 0.01 eV to 1 MeV sterile neutrinos via non-resonant active-sterile flavor oscillations in several pre-BBN cosmologies. We give general equations for models in which the expansion of the Universe is parametrized by its amplitude and temperature power and where entropy is conserved, which include kination and scalar tensor models as special cases.

Contents

1	Introduction	2
2	Early Universe cosmology	4
2.1	Non-standard pre-BBN cosmologies	5
2.2	Kination (K)	5
2.3	Scalar-tensor (ST1 and ST2)	6
2.4	Low reheating temperature (LRT)	7
3	Non-resonant sterile neutrino production	8
3.1	Boltzmann equation	8
3.2	Temperature of maximum non-resonant production	10
3.3	Sterile neutrino momentum distribution functions	12
3.4	Sterile neutrino number densities	12
3.5	Relativistic energy density	16
3.6	Present fraction of the DM in non-resonantly produced sterile neutrinos	17
4	Limits and potential signals	19
4.1	Lyman- α forest WDM and HDM limits	19
4.2	BBN limit on the effective number of neutrino species	20
4.3	Distortions of the CMB spectrum	21
4.4	SN1987A disfavored region	22
4.5	X-ray observations and the 3.5 keV line	23
4.6	Laboratory experiments	24
5	Summary	25
	Acknowledgments	27
A	Additional formulas for non-resonant production	27
A.1	Temperature of maximum rate of production of sterile neutrinos	27
A.2	Momentum distribution functions of non-resonantly produced sterile neutrinos	28
A.3	Relic number density of non-resonantly produced sterile neutrinos	28
A.4	Energy density of non-resonantly produced relativistic sterile neutrinos	30
A.5	Present fraction of the DM in non-resonantly produced sterile neutrinos	32
A.6	DM density limit	33

1 Introduction

The earliest detected cosmological remnants are the light nuclei produced during Big Bang Nucleosynthesis (BBN). The lower limit on the highest temperature of the radiation-dominated epoch in which BBN happened is just close to 5 MeV [1–6]. Thus, the cosmological evolution in the Universe before the temperature of the Universe was 5 MeV is unknown.

Many dark matter (DM) particle candidates are produced before the temperature of the Universe was $T = 5$ MeV, thus assumptions must be made about cosmology in that epoch to compute their relic abundance and momentum distribution. The standard assumptions that are usually made, which constitute the “standard pre-BBN cosmology”, are that the Universe was radiation-dominated and only Standard Model (SM) particles are present. Additionally, it is assumed that no extra entropy in matter and radiation is produced. This is an extension of the known cosmology below 5 MeV to higher temperatures. However, there are cosmological models with alternative assumptions that are equally in agreement with all existing data. This is the case in some well motivated theoretical models, based e.g. on moduli decay, quintessence and extra dimensions. A non-standard cosmological evolution could drastically alter the relic density and momentum distribution of any relics produced before the temperature of the Universe was 5 MeV. Detecting any of these relics would open a new window into this yet unexplored cosmological epoch.

There are three active neutrinos ν_α , characterized by their flavors $\alpha = e, \mu, \tau$, coupled to the W and Z weak gauge bosons¹. These neutrinos are massless within the SM, however, neutrino oscillations [8] show that they are massive. This motivates the study of scenarios with more than three neutrino flavors, as many neutrino mass models include one or more additional “sterile” neutrinos ν_s that do not directly couple to the W and Z bosons.

The theory of active neutrino oscillations has been extensively tested by experimental measurements of neutrino production in the Sun [9–14], in nuclear reactors [15–18], at accelerators [19–23] and in the atmosphere [8, 24]. While the data has been generally consistent with the three-flavor paradigm, several experiments reported anomalies that could be consistently explained by introducing one or more additional sterile neutrinos into the theory with a mass of $m_s = \mathcal{O}(\text{eV})$. In particular, the short-baseline experiments² LSND [25] and MiniBooNE [26] reported excesses of $\bar{\nu}_e$ within $\bar{\nu}_\mu$ beams, and MiniBooNE also found an excess in ν_e appearance [27]. A deficit of ν_e flux from radioactive calibration sources has been observed in gallium experiments³ [29, 30]. Furthermore, an under-abundance of $\bar{\nu}_e$ has

¹Measurements of the invisible decay width of the Z boson limit the number of weakly interacting neutrino species with mass below 45 GeV to three [7].

²In short-baseline experiment the detectors are located at less than 1 km away from the source.

³Recent re-evaluations of gallium cross-sections indicate a weaker sterile neutrino preference [28].

been reported in reactor neutrino experiments⁴ [33]. Additionally, combined fits [34–36] to recent reactor neutrino results by the DANSS [37] and NEOS [38] experiments are consistent with an interpretation based on a sterile neutrino with a mass of $m_s = \mathcal{O}(\text{eV})$ and mixing with a ν_e active neutrino. Reactor neutrino data from the Daya Bay [39], Bugey-3 [40] and PROSPECT [41] experiments constrain these sterile neutrinos and the PTOLEMY [42] and KATRIN [43] experiments will be able to test all or part of this parameter space.

Sterile neutrinos with mass of $\mathcal{O}(\text{keV})$ and a spectrum close to thermal constitute a viable Warm DM (WDM) candidate (see e.g. Ref. [44]). The mass and mixing of sterile neutrinos that make up all or most of the DM is subject to astrophysical constraints, such as those imposed by Lyman- α forest and X-ray observations. If the keV-mass sterile neutrinos are produced from sterile-active oscillations in the early Universe, these limits disfavor them as the sole DM component (see e.g. Ref [45]). These bounds are drastically weakened if sterile neutrinos constitute a sub-dominant DM component (see e.g. Ref. [46]). It has been suggested that the 3.5 keV X-ray emission line observed in 2014 [47, 48] could be produced in the decay of $m_s = 7$ keV sterile neutrinos. The KATRIN laboratory experiment with its proposed TRISTAN upgrade [49], as well as the upcoming HUNTER experiment and its upgrades [50], will test sterile neutrinos in the keV-scale mass range.

If produced in a supernova explosion, sterile neutrinos with mass larger than keV could carry away a sizable fraction of the emitted energy. Asymmetric emission of the sterile neutrinos due to the presence of a strong magnetic field could explain the observed large velocities of pulsars [51]. These effects are independent of the relic abundance of sterile neutrinos and the fraction of the DM they constitute.

Sterile neutrinos without additional interactions beyond the SM that couple to the SM particles only through mixing with active neutrinos, as we assume here, are produced in the early Universe through active-sterile flavor oscillations and collisional processes. For simplicity we assume a ν_s that mixes with only one of the ν_α , which for our figures is ν_e , with a mixing of $\sin \theta$. In the absence of a large lepton asymmetry the oscillations are non-resonant, and the resulting relic number density was first obtained by Dodelson and Widrow [52]. In the standard cosmology this mechanism results in a Fermi-Dirac momentum distribution of sterile neutrinos, with a reduced magnitude with respect to active neutrinos. In the presence of a significant lepton asymmetry in active neutrinos, sterile neutrinos are instead produced via resonant oscillations, as pointed out by Shi and Fuller [53]. Then, the resulting sterile neutrinos have a colder momentum distribution (i.e. with a lower average momentum) that is different from a Fermi-Dirac spectrum. This mechanism was studied in its generality within Ref. [54, 55]. In non-minimal particle models, sterile neutrino production could also proceed via other mechanisms, such as decays of additional heavy scalars [56].

In this work we revisit the effects of different pre-BBN cosmologies on sterile neutrinos with mass $10^{-2} \text{ eV} < m_s < 1 \text{ MeV}$, produced via non-resonant active-sterile oscillations. Sev-

⁴This anomaly has weakened in light of Daya Bay’s reactor fuel cycle measurements [31] and observations of spectral distortions not predicted by flux calculations [32].

eral related studies have been previously carried out [57–59]. We update the older constraints of Ref. [57], extend the results of Ref. [58] – pointing out the significance of upcoming laboratory experiments, and extend the analysis of Ref. [59] on keV-mass neutrinos down to 0.01 eV masses. Here, we provide additional details and further expand on the results presented in our recent letter [60].

In cosmological models in which entropy is conserved the sterile neutrino production depends crucially on the magnitude and temperature dependence of the Hubble expansion rate H . If in the non-standard cosmological phase H is larger than in the standard cosmology, the production of sterile neutrinos during this phase is suppressed. Notably, a particular scalar-tensor model, which was not discussed in the previous study of Ref. [58], allows for a lower expansion rate compared to the standard cosmology and the production is enhanced. We assess the effects of these considerations on the possibility of detecting a sterile neutrino in laboratory experiments. For comparison, we also reconsider low reheating temperature models [57], in which entropy is produced and the radiation bath is subdominant during the non-standard phase. Hence, the dominant sterile neutrino production in this scenario occurs during the late standard cosmological phase.

This paper is organized as follows. In Section 2 we describe a general parametrization for the expansion rate of the Universe H for models in which we assume that the entropy in matter and radiation is conserved. In Section 3 we present the effects of different pre-BBN cosmologies on non-resonant sterile neutrino production. In Section 4 we describe the resulting sterile neutrino limits and regions of interest in mass-mixing space. Finally, in Section 5 we summarize our results.

2 Early Universe cosmology

The expansion rate of the Universe, the Hubble parameter $H = (\dot{a}/a)$ – where a is the cosmological scale factor of the Universe, is determined by the Friedmann equation. In the standard cosmological model [61] the Universe was radiation dominated before BBN, and the highest temperature T of the radiation bath achieved in this epoch is much higher than the temperature $T \simeq 0.8$ MeV at which BBN starts. In the standard cosmology H is

$$H_{\text{Std}} = \sqrt{\frac{8\pi G\rho(T)}{3}} = \left(\frac{T^2}{M_{\text{Pl}}}\right)\sqrt{\frac{8\pi^3 g_*(T)}{90}}. \quad (2.1)$$

Here $\rho(T) = (\pi^2/30)g_*(T)T^4$ is the total energy density, $M_{\text{Pl}} = 1.22 \times 10^{19}$ GeV is the Planck mass and $g_*(T)$ is the number of degrees of freedom contributing to the energy density at temperature T . Assuming that only SM particles are present for T higher than the QCD phase transition at $T \simeq 200$ MeV, we have $g_* = 80$ and it is approximately constant (it reaches $g_* = 100$ at $T \simeq 100$ GeV). Close to the QCD phase transition, the value of g_* decreases steeply with decrement of T , and we take a characteristic value of $g_* \simeq 30$ until T decreases to $T = 20$ MeV. Between this temperature and $T = 1$ MeV, when electrons and positrons

become non-relativistic and annihilate, $g_* = 10.75$ (see e.g. Refs. [62–64]). Unless otherwise stated, for simplicity we use $g_* = 30$ in our figures.

2.1.0 Non-standard pre-BBN cosmologies

The requirement of a successful BBN, which also insures that the subsequent history of the Universe develops as usual, imposes that the Universe is radiation dominated for temperatures $T \lesssim 5$ MeV [1–6]. However, a non-standard cosmological evolution is allowed at higher temperatures.

Any new additional contribution to the energy density in matter or radiation, or equivalently to the geometry sector of Einstein’s equations, results in modification of the Hubble expansion rate through the Friedmann equation. Except for the low reheating temperature model (see below), we consider non-standard cosmologies in which the entropy in matter and radiation is conserved (and hence, the relation between the scale factor of the Universe a and the temperature T follows $a \sim T^{-1}$), but the Hubble expansion H as a function of T is non-standard. In all cosmologies of this type that we will consider H can be given by a simple parameterization [65]

$$H = \eta \left(\frac{T}{T_{\text{tr}}} \right)^\beta H_{\text{Std}} , \quad (2.2)$$

where T_{tr} is a reference temperature, which we identify with the temperature at which before BBN the cosmology transitions to the standard cosmology, η and β are real parameters and η is positive.

To preserve BBN, we require that H_{Std} is recovered in Eq. (2.2) at $T < T_{\text{tr}} = 5$ MeV. Various phenomenological studies of non-standard cosmologies have been carried out [65–69], which can be generally classified by the value of the β parameter: $\beta > 2$ for ultra-fast expansion, e.g. when the Universe is dominated by a field with an exponential potential [70] (as in the ekpyrotic scenario [71]), $\beta = 2$ in the Randall-Sundrum type II brane cosmology [72] (see discussion in Ref. [73]), $\beta = 1$ or larger was considered in “fast-expanding” models in which there is an additional energy density component from a non-interacting component [70], $\beta = 1$ in kination models [68, 73–77], $\beta = 0$ in cosmologies with an overall boost of the Hubble expansion rate, e.g. with a large number of additional relativistic degrees of freedom within the thermal plasma [65], $\beta = -0.8$ can occur in variants of the scalar-tensor cosmology [65, 78] and $\beta = 2/n - 2$ describes $f(R)$ gravity⁵, with $f(R) = R + \text{const.} \times R^n$ [80].

We will provide expressions in terms of η and β for all the relevant equations in our study, but we will focus our discussion on two often considered modified cosmologies, kination (K) and scalar-tensor (ST) models.

2.2.0 Kination (K)

In the kination phase [68, 74–77], the kinetic energy of a scalar field ϕ dominates over its potential energy and all other contributions to the total energy density ρ_{tot} . Hence, it also

⁵For $n = 2$ this reduces to the Starobinsky model [79].

governs the expansion rate in the early Universe. Cosmologies with phases governed by such “fast-rolling” scalar fields can arise in models of quintessence.

During the kination period $\rho_{tot} \simeq \rho_\phi \simeq \dot{\phi}^2/2 \sim a^{-6}$, where ρ_ϕ is the energy density of the scalar ϕ , the associated expansion rate of the Universe during the kination phase is $H_K \sim \sqrt{\rho_{tot}} \sim T^3$. The ratio of ϕ -to-photon energy density at $T \simeq 1$ MeV, $\eta_\phi = \rho_\phi/\rho_\gamma$, fixes the contribution of the ϕ kinetic energy to the total energy density at higher temperatures. Hence, one has $H_K \simeq \sqrt{\eta_\phi}(T/1 \text{ MeV})H_{\text{Std}}$. The value of η_ϕ can be determined by assuming a rapid transition from the kination phase to the radiation dominated phase at the transition temperature T_{tr} , so that $H_K(T_{tr}) = H_{\text{Std}}(T_{tr})$. With this approximation the expansion rate of the Universe during the kination phase is

$$H_K = \left(\frac{T^3}{M_{\text{Pl}}T_{tr}}\right)\sqrt{\frac{8\pi^3 g_*}{90}} = \left(\frac{T}{T_{tr}}\right) H_{\text{Std}} \quad , \quad (2.3)$$

which in Eq. (2.2) corresponds to $\eta = 1$ and $\beta = 1$.

2.3.0 Scalar-tensor (ST1 and ST2)

Scalar-tensor models of gravity [78, 81] have one or more scalar fields coupled through the metric tensor to the matter sector. These extra fields affect the expansion rate of the Universe when the temperature of the thermal bath is higher than the transition temperature T_{tr} , at which a fast transition is assumed to occur before BBN, so that the theory becomes indistinguishable from General Relativity at $T < T_{tr}$. Such scalar-tensor modified cosmologies can appear in models of extra dimensions (e.g. [82]). Depending on the details of the scenario, the respective early Universe expansion rate H_{ST} can be either larger [78] or slightly smaller [83] than the expansion rate within the standard cosmology H_{Std} .

As benchmarks, we consider two scalar-tensor models that are extreme in terms of the magnitude of the expansion rate they predict, which we call ST1 and ST2 and assume $T_{tr} = 5$ MeV. In the ST1 model from Ref. [78] the expansion rate is enhanced compared to the standard cosmology, described by

$$H_{\text{ST1}} = 7.4 \times 10^5 \left(\frac{T_{tr}^{0.8} T^{1.2}}{M_{\text{Pl}}}\right)\sqrt{\frac{8\pi^3 g_*}{90}} = 7.4 \times 10^5 \left(\frac{T}{T_{tr}}\right)^{-0.8} H_{\text{Std}} \quad , \quad (2.4)$$

which in Eq. (2.2) corresponds to $\eta = 7.4 \times 10^5$ and $\beta = -0.8$.

In Ref. [83] it was shown that contributions of an additional “hidden” matter sector beyond the visible sector can result in a reduced expansion rate, compared to the standard cosmology. We choose for ST2 a model of this type with the lowest expansion rate found in Ref. [83], $(H_{\text{ST}}/H_{\text{Std}})^2 = 10^{-3}$, and for which we choose $\beta = 0$ (given the variations in the behavior of H close to T_{tr} of the numerical solutions shown in Fig. 4 of Ref. [83]). Thus

$$H_{\text{ST2}} = 3.2 \times 10^{-2} \left(\frac{1}{M_{\text{Pl}}}\right) T^2 \sqrt{\frac{8\pi^3 g_*}{90}} = 0.03 H_{\text{Std}} \quad , \quad (2.5)$$

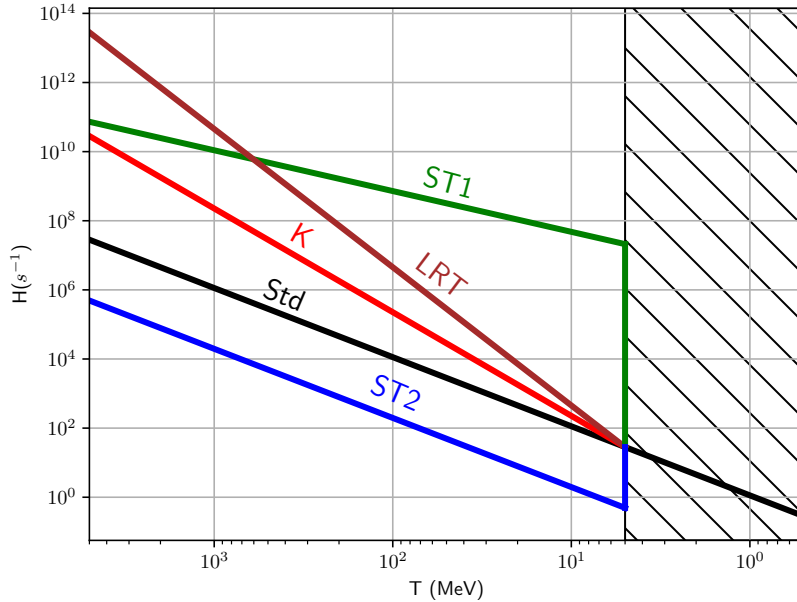


Figure 1: Expansion rate of the Universe H as a function of the temperature T of the radiation bath for the Std (black), K (red), ST1 (green) and ST2 (blue) and LRT (brown) cosmologies. At $T_{tr} = 5$ MeV, the upper boundary of the hatched region, all the non-standard cosmologies transition to the standard cosmology. For simplicity, we assume the transition to be sharp in the ST1 and ST2, cosmologies.

which in Eq. (2.2) corresponds to $\eta = 0.03$ and $\beta = 0$.

Expansion rates in between H_{ST1} and H_{ST2} can also appear within scalar-tensor models and our analysis can be readily applied to them.

Fig. 1 shows the expansion rate of the Universe H as a function of the temperature T of the radiation bath for the Std, H_{Std} (black), K, H_K (red), ST1, H_{ST1} (green), and ST2, H_{ST2} (blue), cosmologies assuming a fast transition at $T_{tr} = 5$ MeV and that for $T < T_{tr}$ the cosmology is standard.

We note that since we impose that non-standard cosmologies transition to the standard cosmology before the onset of BBN, restrictions arising from consistency with current astrophysical observations (e.g. signals from neutron star binary mergers [84]) do not affect our considerations.

2.4.0 Low reheating temperature (LRT)

The phenomenological parametrization of Eq. (2.2) does not capture the whole modification to cosmology in models in which the entropy in radiation and matter is not conserved

and consequently the temperature T dependence on the scale factor a is different than the usual $T \sim 1/a$. One of these is the low reheating temperature (LRT) model.

In the LRT model a scalar field ϕ oscillates coherently around its true minimum and dominates the energy density of the Universe. Decays of ϕ produce a radiation bath that thermalizes to a temperature T and becomes dominant at the reheating temperature T_{RH} . Subsequently, the radiation dominates the energy density of the Universe for $T < T_{\text{RH}}$ (see e.g. Refs. [85, 86]). Such field ϕ could be the inflaton itself or a modulus field producing a late episode of entropy production (see e.g. Ref. [87–92]). Other alternative possibilities include Q-ball decays (e.g. [93]).

In Fig. 1, we show the expansion rate for LRT with $T_{\text{RH}} = T_{\text{tr}} = 5$ MeV in brown.

The LRT scenario may drastically alter the DM relic abundance (see e.g. [57, 85, 86, 94, 95] and discussion in Ref. [66]). The non-resonant production of sterile neutrinos in LRT models was considered in Refs. [57, 95], with the assumption that it predominantly occurs during the standard cosmological phase, when $T < T_{\text{RH}}$, since the thermal bath is subdominant before reheating. This approximation was validated by considering also the production during the non-standard phase in Ref. [94]. Because the non-resonant production rate is far from its maximum for $T < T_{\text{RH}}$, the relic abundance of sterile neutrinos is suppressed in these models. In this study we reconsider the production of sterile neutrinos in LRT model with $T_{\text{RH}} = T_{\text{tr}} = 5$ MeV [57, 94] and update the observational and experimental bounds on them.

3 Non-resonant sterile neutrino production

In the absence of a significant primordial lepton asymmetry, the production of sterile neutrinos happens via non-resonant flavor oscillations between the active neutrinos ν_α of the SM and the sterile neutrino ν_s . This is called the Dodelson-Widrow mechanism (DW) [52] because they derived the analytic solution for the relic number density of sterile neutrinos produced in this manner⁶ (see also earlier work [97, 98]). Interactions of active neutrinos with the surrounding plasma during the oscillations act as measurements and cause the collapse of the wave function into one of the oscillating states, which with some probability results in a sterile neutrino. The production rate is usually not fast enough for sterile neutrinos to equilibrate and the process is a freeze-in of the final abundance.

3.1.0 Boltzmann equation

Assuming that only two neutrinos mix, ν_s and one active neutrino ν_α (which we assume to be ν_e in our figures), the time evolution of the phase-space density distribution function of sterile neutrinos $f_{\nu_s}(p, t)$ with respect to the density function of active neutrinos $f_{\nu_\alpha}(p, t)$

⁶The original Dodelson-Widrow results were subsequently corrected by a factor of 2 [54, 96].

is given by the following Boltzmann equation [54, 61]

$$\begin{aligned} \frac{d}{dt} f_{\nu_s}(p, t) &= \frac{\partial}{\partial t} f_{\nu_s}(p, t) - Hp \frac{\partial}{\partial p} f_{\nu_s}(p, t) \\ &= \Gamma(p, t) \left[f_{\nu_\alpha}(1 - f_{\nu_s}) - f_{\nu_s}(1 - f_{\nu_\alpha}) \right]. \end{aligned} \quad (3.1)$$

Here H is the expansion rate of the Universe, p is the magnitude of the neutrino momentum and $\Gamma(p, t)$ is the conversion rate of active to sterile neutrinos. The active neutrinos are assumed to have a Fermi-Dirac distribution

$$f_{\nu_\alpha} = (e^{\epsilon - \xi} + 1)^{-1}, \quad (3.2)$$

where $E = p$ because all neutrinos we are interested in are relativistic during the production, $\epsilon = p/T$ is the T -scaled dimensionless momentum, and $\xi = \mu_{\nu_\alpha}/T$ is the T -scaled dimensionless chemical potential with μ_{ν_α} being the chemical potential of active ν_α . In the DW mechanism μ_{ν_α} is negligible and so we take $\xi = 0$. Since $f_{\nu_s} \ll 1$, we can ignore Pauli blocking, i.e. $(1 - f_{\nu_s}) = 1$, and while $f_{\nu_s} \ll f_{\nu_\alpha}$ we can also neglect the second term on the right hand side of Eq. (3.1). Changing variables, Eq. (3.1) can be further recast into a more convenient form [54, 58]

$$-HT \left(\frac{\partial f_{\nu_s}(E, T)}{\partial T} \right)_{E/T=\epsilon} \simeq \Gamma(E, T) f_{\nu_\alpha}(E, T), \quad (3.3)$$

where the derivative on the left-hand side is computed at constant ϵ .

The conversion rate Γ is the total interaction rate $\Gamma_\alpha = d_\alpha G_F^2 \epsilon T^3$ of the active neutrinos with the surrounding plasma weighted by the average active-sterile oscillation probability $\langle P_m \rangle$ in matter (see Eq. (6.5) and (6.5) of Ref. [54])

$$\Gamma = \frac{1}{2} \langle P_m(\nu_\alpha \rightarrow \nu_s) \rangle \Gamma_\alpha \simeq \frac{1}{4} \sin^2(2\theta_m) d_\alpha G_F^2 \epsilon T^5. \quad (3.4)$$

In this equation θ_m is the active-sterile mixing angle in matter and d_α is a flavor-dependent parameter, $d_\alpha = 1.13$ for ν_e and $d_\alpha = 0.79$ for ν_μ, ν_τ . Taking into account contributions from the thermal potential V_T and the density potential V_D (that is proportional to the lepton number), the matter mixing angle is given by [54]

$$\sin^2(2\theta_m) = \frac{\sin^2(2\theta)}{\sin^2(2\theta) + \left[\cos(2\theta) - 2\epsilon T(V_D + V_T)/m_s^2 \right]^2}. \quad (3.5)$$

Here, the quantum damping term in the denominator has been omitted, because it is always negligible for the cases we consider.

For DW production, the density potential V_D is assumed to be negligible. The thermal

potential V_T is given by

$$V_T = -B\epsilon T^5, \quad (3.6)$$

where the prefactor B depends on the active neutrino flavor (indicated in parenthesis in the following equation) and on the temperature range (indicated to the right),

$$B = \begin{cases} 10.88 \times 10^{-9} \text{ GeV}^{-4} (e); & 3.02 \times 10^{-9} \text{ GeV}^{-4} (\mu, \tau); & T \lesssim 20 \text{ MeV} \\ 10.88 \times 10^{-9} \text{ GeV}^{-4} (e, \mu); & 3.02 \times 10^{-9} \text{ GeV}^{-4} (\tau); & 20 \text{ MeV} \lesssim T \lesssim 180 \text{ MeV} \\ 10.88 \times 10^{-9} \text{ GeV}^{-4} (e, \mu, \tau); & & T \gtrsim 180 \text{ MeV} \end{cases} \quad (3.7)$$

Since the sterile neutrino production rate $(\partial f_{\nu_s}/\partial T)_\epsilon$ is inversely proportional to the expansion rate H (see Eq. (3.3)), high values of $\eta > 1$ in Eq. (2.2) result in suppressed sterile neutrino production, for fixed m_s and $\sin^2(2\theta)$. Hence, non-standard cosmological models with large $\eta \gg 1$ are less constrained by cosmological and astrophysical upper limits on the relic density, and thus larger active-sterile mixing angles become allowed by these limits. The enlarged open parameter space for the K and ST1 (and also LRT) models places visible sterile neutrinos with $m_s \simeq \text{keV}$ within closer reach of laboratory experiments such as KATRIN [49] and HUNTER [50]. The effect of ST1 is particularly pronounced and there are no astrophysical or cosmological limits on visible ν_s with $m_s \simeq \text{eV}$, which are tested in reactor and accelerator experiments. On the other hand, the ST2 model of Eq. (2.5) with $\eta < 1$ can produce all of the DM at a smaller mixing angle for a given mass than in the standard cosmological scenario.

3.2.0 Temperature of maximum non-resonant production

The sterile neutrino conversion rate Γ , given in Eq. (3.4) and Eq. (3.5), is suppressed at high temperatures by the thermal potential V_T , so that $\Gamma \sim T^{-7}$. At low temperatures, where V_T is negligible, it is suppressed by the decreasing interaction rate, so that $\Gamma \sim T^5$. Where both regimes cross, for cosmologies with $\beta < 2$, the production rate $(\partial f_s/\partial T)_\epsilon$ has a narrow peak as shown in Fig. 2.

The temperature at which the production rate is maximum, T_{max} , depends on $H(T)$, but it does not significantly change for the particular cosmologies we consider (see Fig. 2). This can be seen in Eq. (A.1) where T_{max} is given as a function of β and ϵ , for $\beta \leq 2$. In the standard cosmology the production is maximal when the V_T term is about 0.2 of the mass term (i.e. the square bracket in the denominator of Eq. (3.5) at T_{max} is $[1 - (2\epsilon/m_s^2)T_{\text{max}}V_T(T_{\text{max}})] = [1 + 0.2]$) and is very similar in the other cosmologies.

For the standard cosmology ($\beta = 0$),

$$T_{\text{max}}^{\text{Std}} = 145 \text{ MeV} \left(\frac{m_s}{\text{keV}} \right)^{\frac{1}{3}} \epsilon^{-\frac{1}{3}} \left(\frac{B}{10.88 \times 10^{-9} \text{ GeV}^{-4}} \right)^{-\frac{1}{6}}. \quad (3.8)$$

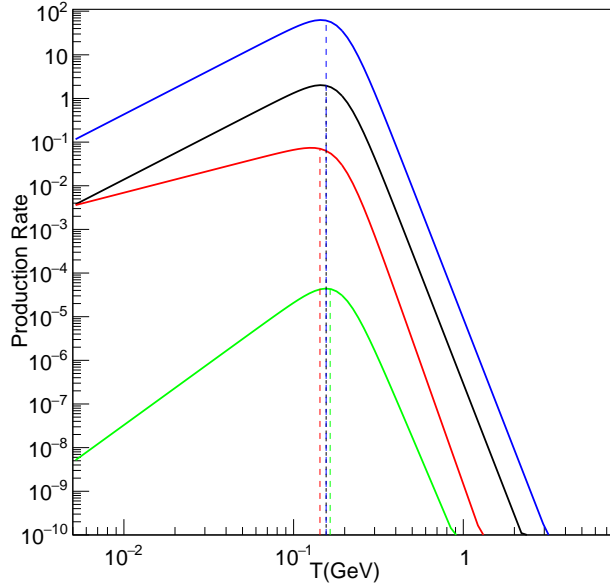


Figure 2: Sterile neutrino non-resonant production rate $(\partial f_{\nu_s}(E, T)/\partial T)_\epsilon$ in Eq. (3.3) as function of the temperature T for $\epsilon = 1$ and $m_s = 1$ keV in the Std (black), K (red), ST1 (green) and ST2 (blue) cosmologies, clearly showing their inverse proportionality with the magnitude of the expansion rate H and also minor differences in shape and width due to the different values of the β parameter. The value of T_{\max} in each case is indicated by a vertical dashed line of the color of the corresponding cosmology.

For ST1 ($\beta = -0.8$) T_{\max} is very similar

$$T_{\max}^{\text{ST1}} = 156 \text{ MeV} \left(\frac{m_s}{\text{keV}} \right)^{\frac{1}{3}} \epsilon^{-\frac{1}{3}} \left(\frac{B}{10.88 \times 10^{-9} \text{ GeV}^{-4}} \right)^{-\frac{1}{6}}. \quad (3.9)$$

Since for ST1 the maximum temperature has an inverse scaling dependence on the momentum via ϵ (because β is negative for this model, see Eq. (A.1)), states with lower momentum will be produced earlier, at higher temperatures.

We note that the usual definition of T_{\max} , as given by Dodelson and Widrow [52], does not depend on ϵ , because it is computed using the production rate integrated over momenta. It coincides with the definition of T_{\max} given here for $\epsilon \simeq 1.3$.

T_{\max}^{K} and T_{\max}^{ST2} for K and ST2 are given in Appendix A.1. They are also very similar.

For non-standard cosmologies with $\beta \geq 2$, the sterile production rate $(\partial f_s/\partial T)_\epsilon$ is continuously increasing with decreasing T , as can be seen in Eq. (A.1) for $\beta = 2$.

3.3.0 Sterile neutrino momentum distribution functions

For the DW production mechanism, a closed-form expression for the momentum distribution function in a non-standard cosmology characterized by H in Eq. (2.2) can be found from Eq. (3.3),

$$f_{\nu_s}(\epsilon) = \int_0^\infty \frac{A'T^{2-\beta}}{(1+B'T^6)^2} f_{\nu_\alpha} dT = A' B'^{(-\frac{1}{2}+\frac{\beta}{6})} \pi \left(\frac{3+\beta}{36}\right) \sec\left(\frac{\beta\pi}{6}\right) f_{\nu_\alpha}(\epsilon), \quad (3.10)$$

where A' and B' are

$$A' = \eta^{-1} \sqrt{\frac{90}{8g_*\pi^3}} M_{\text{Pl}} \Gamma, \quad B' = \frac{2B\epsilon^2}{m_s^2}. \quad (3.11)$$

Replacing in Eq. (3.10) the expressions for A' and B' from Eq. (3.11) and Γ from Eq. (3.4), we obtain the distribution function for generic η and β given in Eq. (A.4) in the Appendix A.2. In the Std cosmology ($\eta = 1, \beta = 0$)

$$f_{\nu_s}^{\text{Std}}(\epsilon) = 9.25 \times 10^{-6} \left(\frac{\sin^2(2\theta)}{10^{-10}}\right) \left(\frac{m_s}{\text{keV}}\right) \left(\frac{g_*}{30}\right)^{-\frac{1}{2}} \left(\frac{d_\alpha}{1.13}\right) \left(\frac{B}{10.88 \times 10^{-9} \text{GeV}^{-4}}\right)^{-\frac{1}{2}} f_{\nu_\alpha}(\epsilon). \quad (3.12)$$

For the ST1 cosmology ($\eta = 7.45 \times 10^5, \beta = -0.8$), the magnitude of the distribution is much smaller than in the Std cosmology,

$$f_{\nu_s}^{\text{ST1}}(\epsilon) = 1.96 \times 10^{-10} \times \epsilon^{-0.27} \left(\frac{\sin^2(2\theta)}{10^{-10}}\right) \left(\frac{m_s}{\text{keV}}\right)^{1.27} \left(\frac{T_{\text{tr}}}{5 \text{MeV}}\right)^{-0.82} \left(\frac{g_*}{30}\right)^{-\frac{1}{2}} \left(\frac{d_\alpha}{1.13}\right) \left(\frac{B}{10.88 \times 10^{-9} \text{GeV}^{-4}}\right)^{-0.64} f_{\nu_\alpha}(\epsilon). \quad (3.13)$$

The distribution functions for the K, ST2 and LRT cosmologies are given in the Appendix A.2.

We can clearly see from Eqs. (3.10) and (3.11), and further in Eq. (A.4), that cosmologies with larger expansion rates (i.e. larger η) require higher mixing angles to produce the same relic density, and vice-versa. For cosmologies with $\beta \neq 0$, there is an extra momentum dependence that makes the distribution warmer (i.e. favors larger ϵ values) for $\beta > 0$ or colder (favors smaller ϵ values) for $\beta < 0$ than the standard Fermi-Dirac.

3.4.0 Sterile neutrino number densities

The number density n_{ν_α} of active neutrinos is obtained by integration over momentum of the distribution function of Eq. (3.2)

$$n_{\nu_\alpha}(T_{\nu_\alpha}) = \left(\frac{3\zeta(3)}{2\pi^2}\right) T_{\nu_\alpha}^3, \quad (3.14)$$

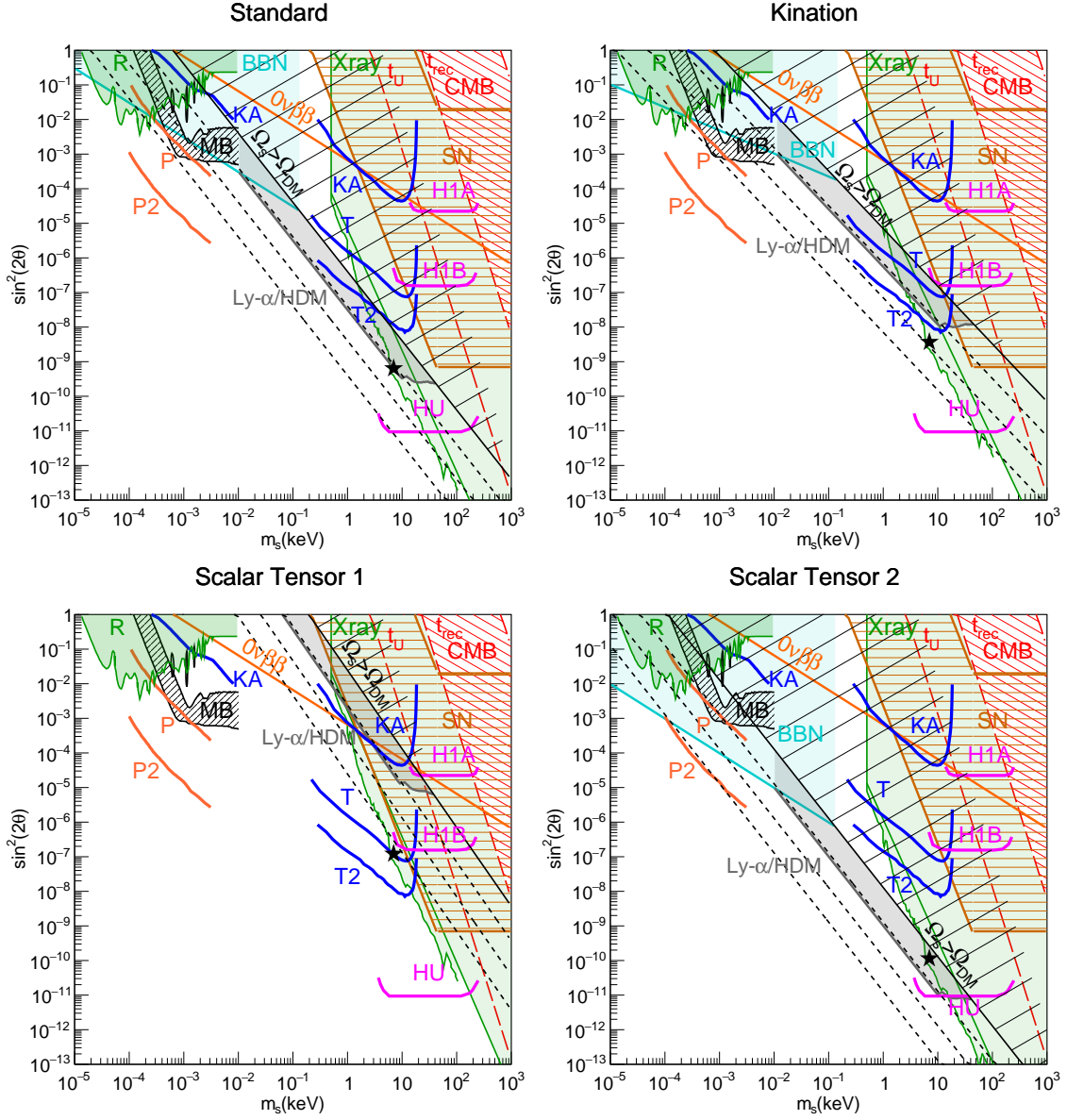


Figure 3: Present relic abundance, limits and regions of interest for standard, kination and scalar-tensor cosmologies. See caption in Fig. 4.

where for photon temperatures $T > 1$ MeV, the temperature of the neutrino background is $T_{\nu_\alpha} = T$, and for $T < 1$ MeV, $T_{\nu_\alpha} = (4/11)T$. The number density n_{ν_s} of sterile neutrinos can be obtained in a similar manner

$$n_{\nu_s}(T_{\nu_s}) = 2 \int_0^\infty \frac{d^3p}{(2\pi)^3} f_{\nu_s}(p) = \frac{T_{\nu_s}^3}{\pi^2} \int_0^\infty d\epsilon \epsilon^2 f_{\nu_s}(\epsilon) = T_{\nu_s}^3 C F_{2+\frac{\beta}{3}}(0), \quad (3.15)$$

considering that active neutrinos have a Fermi-Dirac distribution, as given in Eq. (3.2), with $\xi = 0$ (since for non-resonant production the chemical potential of active neutrinos is negligible) and T_{ν_s} being the temperature of the sterile neutrino background. Here, $C = f_{\nu_s}(\epsilon) \left(\pi^2 \epsilon^{\beta/3} f_{\nu_\alpha}(\epsilon) \right)^{-1}$ is a constant (notice that in Eq. (A.4) f_{ν_s} depends on ϵ only through the product $\epsilon^{\beta/3} f_{\nu_\alpha}(\epsilon)$) and

$$F_k(\xi) = \int_0^\infty dx \frac{x^k}{e^{x-\xi} + 1}, \quad (3.16)$$

is the relativistic Fermi integral. The relic sterile neutrino number density as function of η and β is given in Eq. (A.10).

The term $\beta/3$ in the definition of the index $k = 2 + \beta/3$ comes from the $\epsilon^{\beta/3}$ dependence of f_{ν_s} in Eq. (A.4) (for LRT, the index is instead $k = 3$ because of the ϵ^1 dependence of $f_{\nu_s}^{\text{LRT}}$ in Eq. (A.7)).

The ratio of sterile and active neutrino number densities at the same temperature can be easily stated in terms of the ratio of momentum distributions. For the parametrization of H in Eq. (2.2), this ratio is given in Eq. (A.8).

In the standard cosmology, for which $n_{\nu_s}(T)/n_{\nu_\alpha}(T) = f_{\nu_s}(\epsilon)/f_{\nu_\alpha}(\epsilon)$, the relic sterile neutrino number density is

$$\begin{aligned} n_{\nu_s}^{\text{Std}}(T_{\nu_s}) &= 9.25 \times 10^{-6} \left(\frac{\sin^2 2\theta}{10^{-10}} \right) \left(\frac{m_s}{\text{keV}} \right) \left(\frac{T_{\nu_s}}{T_{\nu_\alpha}} \right)^3 \left(\frac{g_*}{30} \right)^{-\frac{1}{2}} \\ &\times \left(\frac{d_\alpha}{1.13} \right) \left(\frac{B}{10.88 \times 10^{-9} \text{GeV}^{-4}} \right)^{-\frac{1}{2}} n_{\nu_\alpha}(T_{\nu_\alpha}). \end{aligned} \quad (3.17)$$

Thus, the present number density is

$$\begin{aligned} n_{\nu_s}^{\text{Std}} &= 3.74 \times 10^{-4} \text{cm}^{-3} \left(\frac{\sin^2 2\theta}{10^{-10}} \right) \left(\frac{m_s}{\text{keV}} \right) \left(\frac{T_{\nu,0}}{1.95 \text{K}} \right)^3 \\ &\times \left(\frac{g_*}{30} \right)^{-\frac{3}{2}} \left(\frac{d_\alpha}{1.13} \right) \left(\frac{B}{10.88 \times 10^{-9} \text{GeV}^{-4}} \right)^{-\frac{1}{2}}, \end{aligned} \quad (3.18)$$

where $T_{\nu,0} = 1.95 \text{K} = 0.17 \text{meV}$ is the present temperature of the active relic neutrino background.

In the ST1 model, $n_{\nu_s}(T)/n_{\nu_\alpha}(T) = 0.77 e^{0.27} (f_{\nu_s}(\epsilon)/f_{\nu_\alpha}(\epsilon))$, and the number density is significantly reduced for the same mass and mixing angle,

$$\begin{aligned} n_{\nu_s}^{\text{ST1}}(T_{\nu_\alpha}) &= 1.52 \times 10^{-10} \left(\frac{\sin^2 2\theta}{10^{-10}} \right) \left(\frac{m_s}{\text{keV}} \right)^{1.27} \left(\frac{T_{\text{tr}}}{5 \text{MeV}} \right)^{-0.82} \left(\frac{T_{\nu_s}}{T_{\nu_\alpha}} \right)^3 \\ &\times \left(\frac{g_*}{30} \right)^{-\frac{1}{2}} \left(\frac{d_\alpha}{1.13} \right) \left(\frac{B}{10.88 \times 10^{-9} \text{GeV}^{-4}} \right)^{-0.64} n_{\nu_\alpha}(T_{\nu_\alpha}), \end{aligned} \quad (3.19)$$

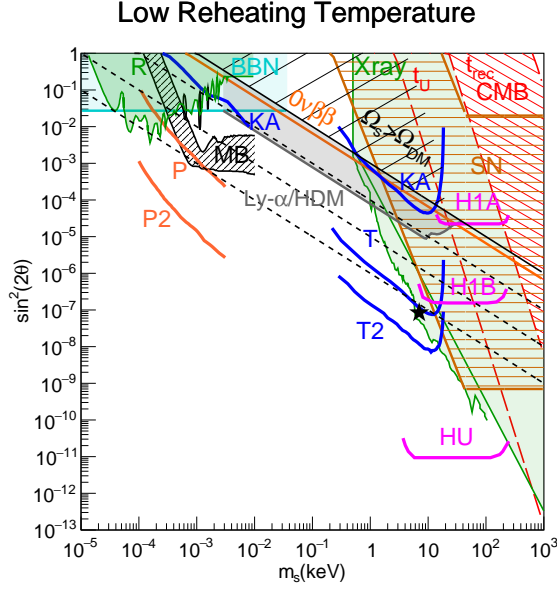


Figure 4: Present relic abundance, limits and regions of interest in the mass-mixing space of a ν_s mixed with ν_e , for LRT cosmology with $T_{RH} = 5$ MeV [57]. Shown are the fraction of the DM in ν_s of 1 (black solid line) and 10^{-1} , 10^{-2} and 10^{-3} (black dotted lines), the forbidden region $\Omega_s/\Omega_{DM} > 1$ (diagonally hatched in black), lifetimes $\tau = t_U$, t_{rec} and t_{th} (see text) of Majorana ν_s (straight long dashed red lines), the region (SN) disfavored by supernovae [99] (horizontally hatched in brown), the location of the 3.5 keV X-ray signal [47, 48] for each cosmology (black star). The regions rejected by reactor neutrino (R) experiments (Daya Bay [39], Bugey-3 [40] and PROSPECT [41]) shown in green, limits on N_{eff} during BBN [100] (BBN) in cyan, Lyman-alpha limits [101] (Ly- α /HDM) in gray, X-ray limits [102–104] including DEBRA [105] (Xray) in green, $0\nu\beta\beta$ decays [106] ($0\nu\beta\beta$) in orange and CMB spectrum distortions [107] (CMB) diagonally hatched in red. Current/future sensitivity of KATRIN (KA) in the keV [49] and eV [43] mass range, its TRISTAN upgrade in 1 yr (T) and in 3 yr (T2) [49] shown by blue solid lines. Magenta solid lines show the reach of the phases 1A (H1A) and 1B (H1B) of HUNTER, and its upgrade (HU) [50]. The $4\text{-}\sigma$ band of compatibility with LSND and MiniBooNE results (MB) in Fig. 4 of [27] is shown densely hatched in black. The three black vertical elliptical contours are the regions allowed at $3\text{-}\sigma$ by DANSS [37] and NEOS [38] data in Fig. 4 of [35]). Orange solid lines show the reach of PTOLEMY for 10 mg-yr (P) and 100 g-yr (P2) exposures (from Figs. 6 and 7 of [42]).

with the present number density being

$$\begin{aligned}
 n_{\nu_s}^{ST1} &= 6.13 \times 10^{-9} \text{ cm}^{-3} \left(\frac{\sin^2 2\theta}{10^{-10}} \right) \left(\frac{m_s}{\text{keV}} \right)^{1.27} \left(\frac{T_{tr}}{5 \text{ MeV}} \right)^{-0.82} \left(\frac{T_{\nu,0}}{1.95 \text{ K}} \right)^3 \\
 &\times \left(\frac{g_*}{30} \right)^{-\frac{3}{2}} \left(\frac{d_\alpha}{1.13} \right) \left(\frac{B}{10.88 \times 10^{-9} \text{ GeV}^{-4}} \right)^{-0.64}. \quad (3.20)
 \end{aligned}$$

Here, g_* is the number of relativistic degrees of freedom when sterile neutrinos are produced, which we take to be $g_*(T_{\text{max}})$. Thus, at present, the ratio of temperatures of the sterile and active neutrinos is $(T_{\nu_s,0}/T_{\nu,0}) = (10.75/g_*)^{1/3}$.

The present number densities for the K and ST2 and also LRT cosmologies are given in the Appendix A.3.

3.5.0 Relativistic energy density

The energy density of relativistic active neutrinos is given by (Eq. (3.2))

$$\rho_{\nu_\alpha} = 2 \int_0^\infty \frac{d^3p}{(2\pi)^3} p f_{\nu_\alpha}(p) = \frac{T^4}{\pi^2} \int_0^\infty d\epsilon \epsilon^3 f_{\nu_\alpha}(\epsilon) = \frac{T^4}{\pi^2} F_3(0), \quad (3.21)$$

where the Fermi integral $F_k(\xi)$ is defined in Eq. (3.16). Similarly, the energy density of relativistic sterile neutrinos is

$$\rho_{\nu_s} = 2 \int_0^\infty \frac{d^3p}{(2\pi)^3} p f_{\nu_s}(p) = \frac{T^4}{\pi^2} \int_0^\infty d\epsilon \epsilon^3 f_{\nu_s}(\epsilon) = T^4 C F_{3+\frac{\beta}{3}}(0). \quad (3.22)$$

To obtain the last equality we used the momentum distributions for the models with H given in Eq. (2.2). The resulting energy density in terms of the parameters η and β is given in Eq. (A.19).

For the LRT model, the index in the function F_k in this equation is not $k = 3 + \beta/3$ but instead $k = 4$ because of the ϵ dependence of $f_{\nu_s}^{\text{LRT}}$ in Eq. (A.7).

The ratio of sterile and active neutrino relic densities at the same temperature T can be easily stated in terms of the ratio of momentum distributions. This ratio is given in terms of η and β in Eq. (A.17).

In the Std cosmology, $\rho_{\nu_s}(T)/\rho_{\nu_\alpha}(T) = n_{\nu_s}(T)/n_{\nu_\alpha}(T) = f_{\nu_s}(\epsilon)/f_{\nu_\alpha}(\epsilon)$, and the energy density of non-resonantly produced relativistic sterile neutrinos with temperature T_{ν_s} is

$$\begin{aligned} \rho_{\nu_s}^{\text{Std}}(T_{\nu_s}) &= 9.25 \times 10^{-6} \left(\frac{\sin^2 2\theta}{10^{-10}} \right) \left(\frac{m_s}{\text{keV}} \right) \left(\frac{T_{\nu_s}}{T_{\nu_\alpha}} \right)^4 \left(\frac{g_*}{30} \right)^{-\frac{1}{2}} \\ &\times \left(\frac{d_\alpha}{1.13} \right) \left(\frac{B}{10.88 \times 10^{-9} \text{ GeV}^{-4}} \right)^{-\frac{1}{2}} \rho_{\nu_\alpha}(T_{\nu_\alpha}), \end{aligned} \quad (3.23)$$

or,

$$\begin{aligned} \rho_{\nu_s}^{\text{Std}}(T_{\nu_s}) &= 6.93 \times 10^{26} \frac{\text{MeV}}{\text{cm}^3} \left(\frac{\sin^2 2\theta}{10^{-10}} \right) \left(\frac{m_s}{\text{keV}} \right) \left(\frac{T_{\nu_s}}{1 \text{ MeV}} \right)^4 \left(\frac{g_*}{30} \right)^{-\frac{1}{2}} \\ &\times \left(\frac{d_\alpha}{1.13} \right) \left(\frac{B}{10.88 \times 10^{-9} \text{ GeV}^{-4}} \right)^{-\frac{1}{2}}. \end{aligned} \quad (3.24)$$

For ST1 instead, $\rho_{\nu_s}(T)/\rho_{\nu_a}(T) = 0.92(n_{\nu_s}(T)/n_{\nu_a}(T))$ and the density is much smaller

$$\begin{aligned} \rho_{\nu_s}^{\text{ST1}}(T_{\nu_s}) &= 1.39 \times 10^{-10} \left(\frac{\sin^2 2\theta}{10^{-10}} \right) \left(\frac{m_s}{\text{keV}} \right)^{1.27} \left(\frac{T_{\text{tr}}}{5 \text{ MeV}} \right)^{-0.82} \left(\frac{T_{\nu_s}}{T_{\nu_\alpha}} \right)^4 \left(\frac{g_*}{30} \right)^{-\frac{1}{2}} \\ &\times \left(\frac{d_\alpha}{1.13} \right) \left(\frac{B}{10.88 \times 10^{-9} \text{ GeV}^{-4}} \right)^{-0.64} \rho_{\nu_\alpha}(T_{\nu_\alpha}), \end{aligned} \quad (3.25)$$

or,

$$\begin{aligned} \rho_{\nu_s}^{\text{ST1}}(T_{\nu_s}) &= 1.04 \times 10^{22} \frac{\text{MeV}}{\text{cm}^3} \left(\frac{\sin^2 2\theta}{10^{-10}} \right) \left(\frac{m_s}{\text{keV}} \right)^{1.27} \left(\frac{T_{\text{tr}}}{5 \text{ MeV}} \right)^{-0.82} \left(\frac{T_{\nu_s}}{1 \text{ MeV}} \right)^4 \left(\frac{g_*}{30} \right)^{-\frac{1}{2}} \\ &\times \left(\frac{d_\alpha}{1.13} \right) \left(\frac{B}{10.88 \times 10^{-9} \text{ GeV}^{-4}} \right)^{-0.64}. \end{aligned} \quad (3.26)$$

The relativistic energy density $\rho_{\nu_s}^{\text{K}}$, $\rho_{\nu_s}^{\text{ST2}}$ and $\rho_{\nu_s}^{\text{LRT}}$ for the K, ST2 and LRT cosmologies are given in Appendix A.4.

These expressions apply after the bulk of the sterile neutrinos has been produced and while they are relativistic: $m_s < T < T_{\text{max}}$ (or for $m_s < T < T_{\text{RH}}$ in LRT models).

The average T -scaled dimensionless sterile neutrino momentum $\langle \epsilon \rangle$ in the different cosmologies is given in terms of the parameters η and β in Eq. (2.2) for $T_{\text{tr}} = 5 \text{ MeV}$ is

$$\langle \epsilon \rangle = \frac{\rho_{\nu_s}(T)}{T n_{\nu_s}(T)} = \frac{F_{3+\beta/3}(0)}{F_{2+\beta/3}(0)} = \begin{cases} 3.15, & \text{Std} \\ 3.47, & \text{K} \\ 2.89, & \text{ST1} \\ 3.15, & \text{ST2} \end{cases} \quad (3.27)$$

where $F_k(\xi)$ is given in Eq. (3.16) as before. For the LTR model with $T_{\text{RH}} = 5 \text{ MeV}$

$$\langle \epsilon \rangle = \frac{\rho_{\nu_s}(T)}{T n_{\nu_s}(T)} = \frac{F_4(0)}{F_3(0)} = 4.11, \quad \text{LRT} \quad (3.28)$$

3.6.0 Present fraction of the DM in non-resonantly produced sterile neutrinos

The present sterile neutrino relic density must not exceed the DM density, i.e. $\Omega_{\nu_s} = \rho_{\nu_s}/\rho_{\text{crit}} \leq \Omega_{\text{DM}} = \rho_{\text{DM}}/\rho_{\text{crit}}$, where $\Omega_{\text{DM}} h^2 = 0.1186 \simeq 0.12$, $\rho_{\text{crit}} = 1.054 \times 10^{-5} h^2 \text{ GeV}/\text{cm}^3$ is the critical density of the Universe and $h = 0.678$ [100]. Hence, the fraction of the DM consisting of sterile neutrinos $f_{s,\text{DM}} = \rho_{\nu_s}/\rho_{\text{DM}}$ must be $f_{s,\text{DM}} \leq 1$.

At present, all the sterile neutrinos we consider (i.e. all neutrinos with $m_s > 10^{-2} \text{ eV}$), are non-relativistic, thus $\rho_{\nu_s,0} = m_s n_{\nu_s,0}$. Hence, the present fraction of the DM in sterile neutrinos is $f_{s,\text{DM}} = (n_{\nu_s,0} m_s / \rho_{\text{DM}})$. This fraction is given as a function of the η and β

parameters in Eq. (A.25). In the Std cosmology this fraction is

$$\begin{aligned}
f_{s,\text{DM}}^{\text{Std}} &= \left(\frac{n_{\nu_s,0} m_s}{\rho_{\text{DM}}} \right)^{\text{Std}} = \\
&= 2.48 \times 10^{-4} \left(\frac{\sin^2(2\theta)}{10^{-10}} \right) \left(\frac{m_s}{\text{keV}} \right)^2 \left(\frac{T_{\nu,0}}{1.95 \text{ K}} \right)^3 \\
&\quad \times \left(\frac{g_*}{30} \right)^{-\frac{3}{2}} \left(\frac{d_\alpha}{1.13} \right) \left(\frac{\Omega_{\text{DM}} h^2}{0.12} \right) \left(\frac{B}{10.88 \times 10^{-9} \text{ GeV}^{-4}} \right)^{-\frac{1}{2}}
\end{aligned} \tag{3.29}$$

and in the ST1 cosmology is instead

$$\begin{aligned}
f_{s,\text{DM}}^{\text{ST1}} &= \left(\frac{n_{\nu_s,0} m_s}{\rho_{\text{DM}}} \right)^{\text{ST1}} = \\
&= 4.09 \times 10^{-9} \left(\frac{\sin^2(2\theta)}{10^{-10}} \right) \left(\frac{m_s}{\text{keV}} \right)^{2.27} \left(\frac{T_{\text{tr}}}{5 \text{ MeV}} \right)^{-0.82} \left(\frac{T_{\nu,0}}{1.95 \text{ K}} \right)^3 \\
&\quad \times \left(\frac{g_*}{30} \right)^{-\frac{3}{2}} \left(\frac{d_\alpha}{1.13} \right) \left(\frac{\Omega_{\text{DM}} h^2}{0.12} \right) \left(\frac{B}{10.88 \times 10^{-9} \text{ GeV}^{-4}} \right)^{-0.64}.
\end{aligned} \tag{3.30}$$

The present sterile neutrino fraction of the DM for K, ST2 and also the LRT cosmologies are given in Appendix A.5.

The condition $f_{s,\text{DM}} = 1$ defines the mixing we call $\sin^2(2\theta)_{\text{DW,lim}}$ as a function of m_s . In the log-log scales used in our figures, this is a straight line on which sterile neutrinos account for the entirety of the DM. As a function of η and β , $\sin^2(2\theta)_{\text{DW,lim}}(m_s)$ is given in Eq. (A.29).

In the Std cosmology

$$\begin{aligned}
\sin^2(2\theta)_{\text{DW,lim}}^{\text{STD}} &= 4.02 \times 10^{-7} \left(\frac{m_s}{\text{keV}} \right)^{-2} \left(\frac{T_{\nu,0}}{1.95 \text{ K}} \right)^{-3} \left(\frac{g_*}{30} \right)^{\frac{3}{2}} \left(\frac{d_\alpha}{1.13} \right)^{-1} \\
&\quad \times \left(\frac{\Omega_{\text{DM}} h^2}{0.12} \right)^{-1} \left(\frac{B}{10.88 \times 10^{-9} \text{ GeV}^{-4}} \right)^{\frac{1}{2}}
\end{aligned} \tag{3.31}$$

and in the ST1 cosmology

$$\begin{aligned}
\sin^2(2\theta)_{\text{DW,lim}}^{\text{ST1}} &= 2.46 \times 10^{-2} \left(\frac{m_s}{\text{keV}} \right)^{-2.27} \left(\frac{T_{\text{tr}}}{5 \text{ MeV}} \right)^{0.82} \left(\frac{T_{\nu,0}}{1.95 \text{ K}} \right)^{-3} \left(\frac{g_*}{30} \right)^{\frac{3}{2}} \\
&\quad \times \left(\frac{d_\alpha}{1.13} \right)^{-1} \left(\frac{\Omega_{\text{DM}} h^2}{0.12} \right)^{-1} \left(\frac{B}{10.88 \times 10^{-9} \text{ GeV}^{-4}} \right)^{0.64}.
\end{aligned} \tag{3.32}$$

In Appendix A.6 this function is given for the K and ST2 cosmologies, and also for the LRT (see Eq. (A.32)).

In Figs. 3 and 4, the fractions $f_{s,\text{DM}} = 1$ is indicated with a solid black lines and $f_{s,\text{DM}} = 10^{-1}, 10^{-2}, 10^{-3}$ are indicated with dotted black lines.

4 Limits and potential signals

Here we discuss constraints, regions of interest in the mass-mixing plane and potential signals for sterile neutrinos produced via non-resonant active-sterile oscillations in different pre-BBN cosmologies. The results are shown in Figs. 3 and 4. In the figures we assume that the sterile neutrino only mixes with ν_e .

The most stringent cosmological and astrophysical limits on sterile neutrinos come from Lyman- α forest and X-ray observations for the 1 to 10 keV mass range and BBN for $m_s < 100$ eV. We also discuss the 3.5 keV X-ray line as well as upcoming laboratory experiments such as KATRIN/TRISTAN [49] and HUNTER [50] for the 1 to 10 keV mass range, reactor and accelerator neutrino experiments for $m_s < 10$ eV and also the $0\nu\beta\beta$ searches.

4.1.0 Lyman- α forest WDM and HDM limits

Sterile neutrinos of $m_s = \mathcal{O}(\text{keV})$ produced non-resonantly constitute a warm DM (WDM) candidate. The free-streaming of DM particles suppresses structure formation below the free-streaming scale (see e.g. Ref. [44])

$$\lambda_{\text{fs}} = a(t_U) \int_{t_i}^{t_U} dt' \frac{v(t')}{a(t')} \simeq 1 \text{ Mpc} \left(\frac{\text{keV}}{m_s} \right) \frac{\langle p_{\nu_s} \rangle}{\langle p_{\nu_\alpha} \rangle} = 1 \text{ Mpc} \left(\frac{\langle \epsilon \rangle}{3.15} \right) \left(\frac{\text{keV}}{m_s} \right) \frac{T_{\nu_s}}{T_{\nu,0}}, \quad (4.1)$$

where $v(t)$ is a typical DM velocity, t_U is the present lifetime of the Universe, t_i is some initial very early time whose exact value is not important, $a(t)$ is the scale factor of the Universe, $\langle p_{\nu_s} \rangle$ and $\langle p_{\nu_\alpha} \rangle$ are the average absolute values of the sterile and active neutrino momentum and T_{ν_s} and $T_{\nu,0}$ are the present temperatures of the sterile and active neutrinos, respectively.

Observations of the Lyman- α forest⁷ in the spectra of distant quasars constrain the power spectrum on $\sim 0.1 - 1$ Mpc scales [101], which from Eq. (4.1) constrains WDM and thus sterile neutrinos with $m_s = \mathcal{O}(\text{keV})$.

The Lyman- α limits are usually given in terms of the mass m_{therm} of a fermion that was in thermal equilibrium at some point in the history of the Universe, and thus has a Fermi-Dirac spectrum, and thus has $\langle \epsilon \rangle = 3.15$, and a temperature T_{therm} that depends on when the fermion decoupled from the radiation bath. Hence, the relic density Ω_{therm} of this thermal fermion, which depends on its temperature and mass, and its mass are free independent parameters. Sterile neutrinos produced via active-sterile oscillations do not have a thermal equilibrium spectrum, and could have $\langle \epsilon \rangle \neq 3.15$ (see Eqs. (3.27) and (3.28)). Sterile neutrinos may also have a temperature T_{ν_s} smaller than the active neutrino temperature T_ν . In fact, for $m_s = \mathcal{O}(\text{keV})$ the temperature of maximum production $T_{\text{max}} > 100$ MeV (except in the LRT models) is much higher than the active neutrino decoupling temperature $T \simeq 3$ MeV, resulting in $T_{\nu_s} < T_\nu$.

⁷An alternative approach is to use DM halo counts, whose number and formation are also related to free-streaming scales (see the discussion in Ref. [44]).

Following Ref. [108], we equate the free-streaming scales of thermal WDM and sterile neutrinos

$$\frac{\langle \epsilon \rangle T_{\nu_s}}{m_s} = \frac{3.15 T_{\text{therm}}}{m_{\text{therm}}}, \quad (4.2)$$

as well as their energy densities, $\Omega_{\text{therm}} = \Omega_{\nu_s} = f_{s,\text{DM}} \Omega_{DM}$. This allows to identify the sterile neutrino mass that would result in the same free-streaming as a thermal WDM fermion with mass m_{therm}

$$m_s = 4.46 \text{ keV} \left(\frac{\langle \epsilon \rangle}{3.15} \right) \left(\frac{m_{\text{therm}}}{\text{keV}} \right)^{\frac{4}{3}} \left(\frac{T_{\nu_s}}{T_{\nu_\alpha}} \right) \left(\frac{0.12}{f_{s,\text{DM}} \Omega_{DM} h^2} \right)^{\frac{1}{3}}, \quad (4.3)$$

where $T_{\nu_s}/T_{\nu_\alpha} = (10.75/g_*)^{1/3}$. For our figures we use $g_* = 30$ except for the LRT cosmology for which we take $g_* = 15$.

The Lyman- α bounds of Ref. [101] on m_{therm} can now be translated into bounds on m_s through Eq. (4.3). We use the 2- σ bounds from the right panel of Fig. 6 of Ref. [101] coming from SDSS, XQ and HR data. These limits impose that sterile neutrinos do not account for more than $\sim 8\%$ of the DM density for $m_s \lesssim 1$ keV. Lower m_s values yield larger free-streaming lengths, which for $\lambda_{\text{fs}} \gtrsim 1$ Mpc scales will not significantly alter the Lyman- α bounds. Hence, in Figs. 3 and 4 we extend the saturated bound of Ref. [101] to lighter sterile neutrinos that would constitute Hot DM (HDM), until it is superseded by the BBN bound in Eq. (4.7).

4.2.0 BBN limit on the effective number of neutrino species

The impact on BBN of an increased expansion rate of the Universe yields an upper limit on N_{eff} , the effective number of relativistic active neutrino species present during BBN. Assuming that only sterile neutrinos and SM active neutrinos contribute to N_{eff} ,

$$N_{\text{eff}} = 3.045 + \left(\frac{\rho_{\nu_s}}{\rho_{\nu_\alpha}} \right), \quad (4.4)$$

where 3.045 is the contribution of the SM active neutrinos alone [109, 110]. All the sterile neutrinos we consider are relativistic during BBN, thus $(\rho_{\nu_s}/\rho_{\nu_\alpha})$ is the ratio during BBN of the relativistic energy densities of the sterile neutrino, $\rho_{\nu_s} = \langle \epsilon \rangle T n_{\nu_s}$ with $\langle \epsilon \rangle$ given in Eq. (3.27), and one active neutrino species ν_α , $\rho_{\nu_\alpha} = 3.15 T n_{\nu_\alpha}$ ⁸. Hence,

$$\Delta N_{\text{eff}} = N_{\text{eff}} - 3.045 \simeq \left(\frac{\langle \epsilon \rangle}{3.15} \right) \left(\frac{10.75}{g_*} \right)^{1/3} \left(\frac{n_{\nu_s}}{n_{\nu_\alpha}} \right). \quad (4.5)$$

⁸We note that only for neutrinos much heavier than those we consider here sterile neutrinos could decay before BBN, thus increasing N_{eff} due to their decay products (heavy sterile neutrinos have been recently suggested as a solution to the observed tension between local and early Universe measurements of the Hubble constant [111]).

Here, the ratio n_{ν_s}/n_{ν_α} in each cosmology (see Sec. 3.4 and Appendix A.3 for sterile neutrinos produced non-resonantly) is the same during BBN and at present, since both the number densities of sterile and of active neutrinos just redshift for $T < 1$ MeV (and BBN starts at about $T = 0.8$ MeV). Using Eq. (3.14), the present number density of one active neutrino is

$$n_{\nu_\alpha} \simeq 112 \text{ cm}^{-3} \left(\frac{T_{\nu,0}}{1.95 \text{ K}} \right)^3. \quad (4.6)$$

The BBN upper bound of $N_{\text{eff}} < 3.4$ at 95% confidence level [100] through the Eq. (4.5) rejects the cyan region in mass-mixing labelled “BBN” in Figs. 3 and 4. This upper limit is similar to the Planck 2018 limit [112] derived from cosmic microwave background radiation (CMB) data on N_{eff} . However, the CMB limit applies only to neutrinos that are relativistic during recombination, i.e. whose mass is $m_s \ll 1$ eV. Thus, the limit would apply only to a small region of the large parameter space we consider and hence we do not include it. In addition, the limits imposed on the effective sterile mass $m_{s,\text{eff}}$ or the sum of active neutrino masses [112, 113] by Planck 2018, BICEP2/Keck and BAO data do not significantly change those we obtained based on N_{eff} during BBN and thus we do not include them either. Earlier Planck limits on both N_{eff} and $m_{s,\text{eff}}$ were considered in a previous related study of Ref. [58].

Alternatively to obtaining the limit from Eq. (4.5), we can use the same equation to derive a limit on the present fraction of the DM consisting of sterile neutrinos. The present value of the number density $n_{\nu_s,0}$ determines the present relic density $\rho_{s,0} = n_{\nu_s,0}m_s$ and thus the present fraction of the DM in sterile neutrinos corresponding to a particular ΔN_{eff} :

$$f_{s,\text{DM}} = \frac{n_{\nu_s,0}m_s}{\rho_{\text{DM}}} = 35.5 \left(\frac{\langle \epsilon \rangle}{3.15} \right)^{-1} \left(\frac{m_s}{\text{keV}} \right) \left(\frac{T_{\nu,0}}{1.95 \text{ K}} \right)^3 \left(\frac{g_*}{10.75} \right)^{\frac{1}{3}} \left(\frac{\Omega_{\text{DM}}h^2}{0.1198} \right)^{-1} \left(\frac{\Delta N_{\text{eff}}}{0.4} \right), \quad (4.7)$$

where g_* is the number of entropy degrees of freedom when ν_s are produced. Using Eq. (A.19) for $f_{s,\text{DM}}$, or the equation corresponding to a particular cosmological model, $\Delta N_{\text{eff}} < 0.4$ imposes an upper limit on the fraction of the DM consisting of sterile neutrinos.

4.3.0 Distortions of the CMB spectrum

Photons produced in the decays of sterile neutrinos before recombination, i.e. $\tau < t_{\text{rec}} \simeq 1.2 \times 10^{13}$ sec, can distort the CMB spectrum [114, 115] if they are produced after the thermalization time $t_{\text{th}} \simeq 10^6$ sec (see e.g. the discussion in Ref. [95]). Lifetimes of Majorana sterile neutrinos⁹ equal to the lifetime of the Universe, $t_U = 4.36 \times 10^{17}$ sec, to t_{rec} and to t_{th} are indicated with red long-dashed straight lines in Figs. 3 and 4. The COBE FIRAS limits [107] on distortions of the CMB spectrum reject lifetimes $t_{\text{rec}} > \tau > t_{\text{th}}$ (region diagonally hatched in red in Figs. 3 and 4 labeled “CMB”).

Non-thermal photons produced before the thermalization time t_{th} are rapidly incorporated into the Planck spectrum through processes that change the number of photons, such

⁹For Dirac neutrinos the lifetime must be multiplied by 2.

as double Compton scattering ($\gamma e \rightarrow \gamma \gamma e$), which are no longer effective after t_{th} . For $t_{\text{th}} < \tau_s < 10^9$ sec, photon number preserving processes, such as elastic Compton scattering, are still efficient. These processes thermalize the photons into a Bose-Einstein spectrum with a non-zero photon chemical potential μ . If the initial spectrum has fewer photons than a black body of the same total energy the chemical potential is positive and $\mu > 0$ (if instead it has more photons, $\mu < 0$). For $|\mu| \ll 1$, the only values of μ allowed by the COBE satellite limit $|\mu| < 0.9 \times 10^{-4}$ at the 95% CL [107], the energy released into photons in the decay is [114]

$$\frac{\Delta\rho_\gamma}{\rho_\gamma} \simeq 0.714\mu . \quad (4.8)$$

For longer lifetimes, the photon number preserving processes can no longer establish a Bose-Einstein spectrum. Thus, for $10^9 \text{ sec} < \tau_s < t_{\text{rec}}$ the energy released into photons by the decays is not thermalized but still heats up the electrons. Through inverse-Compton scattering this produces a distorted spectrum characterized by a parameter y . The COBE bound on this parameter is $|y| < 1.5 \times 10^{-5}$ [107] and, for $|y| \ll 1$, y is related to the energy released in non-thermal photons as [114]

$$\frac{\Delta\rho_\gamma}{\rho_\gamma} \simeq 4y . \quad (4.9)$$

Coincidentally, the upper limits on μ and y are such that in both cases, Eqs. (4.8) and (4.9), the upper limit on the fractional increase in the photon energy density due to the decay of the sterile neutrinos is 6×10^{-5} . Thus, assuming that the decays happen instantaneously at $t = \tau_s$, and noting that the energy of each photon produced in a decay is $m_s/2$, $\rho_\gamma = 2.7 T n_\gamma$, the temperature-time relation is $T \simeq \text{MeV} (t/\text{sec})^{1/2}$, we have

$$\frac{\Delta\rho_\gamma}{\rho_\gamma} = \frac{B (m_s/2) n_{\nu_s}}{2.7 T n_\gamma} \simeq \frac{(B/2) m_s n_{\nu_s}}{2.7 \text{MeV} n_\gamma} \left(\frac{\tau_s}{\text{sec}} \right)^{1/2} \simeq \frac{(B/2) f_{s,\text{DM}} \rho_{\text{DM}}}{2.7 \text{MeV} n_\gamma} \left(\frac{\tau_s}{\text{sec}} \right)^{1/2} \lesssim 6 \times 10^{-5} . \quad (4.10)$$

Here B is the branching ratio for the radiative decay, so that $B n_{\nu_s}$ is the number of photons produced when the sterile neutrinos decay, the ratio (n_{ν_s}/n_γ) is the same for any $T < 1$ MeV, and at present the energy density in sterile neutrinos is $n_{\nu_s} m_s = f_{s,\text{DM}} \rho_{\text{DM}}$. In our case the branching ratio is $B = 0.78 \times 10^{-2}$, and at present $n_\gamma = 413/\text{cm}^3$ and $\rho_{\text{DM}} \simeq 1.25 \text{ keV}/\text{cm}^3$, thus we get

$$f_{s,\text{DM}} \left(\frac{\tau_s}{t_{\text{rec}}} \right)^{1/2} \lesssim 4 \times 10^{-3} . \quad (4.11)$$

This mean that for $\tau = 10^6$ the limit is $f_{s,\text{DM}} < 12$. We can easily see in Figs. 3 and 4 that the values of the fraction $f_{s,\text{DM}}$ of the DM in sterile neutrinos are much larger than the upper limit in the whole lifetime range $t_{\text{rec}} > \tau > t_{\text{th}}$ where the limit applies.

4.4.0 SN1987A disfavored region

The energy loss due to sterile neutrinos produced in core collapse supernovae explosions disfavors [99] the region horizontally hatched in brown and labeled ‘‘SN’’ in Figs. 3 and 4. Due

to the considerable uncertainty in the neutrino transport and flavor transformation within hot and dense nuclear matter [54], it is difficult to exclude this region entirely. Recent studies regarding sterile neutrinos mixing with ν_μ or ν_τ have been carried out in e.g. Ref. [116, 117].

4.5.0 X-ray observations and the 3.5 keV line

The most restrictive limits on sterile neutrinos with mass $m_s = 1 - 10$ keV come from astrophysical indirect detection searches of X-rays produced in their $\nu_s \rightarrow \nu_\alpha \gamma$ two-body decay¹⁰ [102–104]. The rate of this decay mode is [118, 119]

$$\Gamma_\gamma = 1.38 \times 10^{-32} \text{ s}^{-1} \left(\frac{\sin^2(2\theta)}{10^{-10}} \right) \left(\frac{m_s}{\text{keV}} \right)^5. \quad (4.12)$$

Due to the rapid decrease of the decay rate with decreasing m_s , X-ray observations do not provide meaningful constraints for sterile neutrinos with $m_s < 1$ keV.

The model independent X-ray bounds found in the literature [102–104] assume that sterile neutrinos constitute the entirety of the DM. In order to translate the published limits into those that apply in our scenarios we take into account that the X-ray signal depends on the produced photon flux, thus the limits actually constrain the product $(\Omega_s/\Omega_{\text{DM}}) \sin^2 2\theta$ and not just $\sin^2 2\theta$. The present sterile neutrino fraction $f_{s,\text{DM}} = (\Omega_s/\Omega_{\text{DM}})$ of the DM is itself proportional to $\sin^2 2\theta$ (because of the dependence of n_{ν_s} in Eq. (A.10), and Sec. 3.4 and Appendix A.3 on the mixing). Hence, the X-ray limits shown in Fig. 3 are related to the published model independent X-ray bounds through a simple rescaling.

From Eq. (A.25), DM fraction in sterile neutrinos can be written for non-resonant production as $f_{s,\text{DM}} = \sin^2(2\theta)/\sin^2(2\theta)_{\text{DW,lim}}$, thus the constraint on our models is the geometric mean of the published model independent limit and $\sin^2(2\theta)_{\text{DW,lim}}$ (given in Eq. (3.31), Eq. (3.32) and Appendix A.6 for the different cosmologies we consider).

The same rescaling applies to upper limits on the diffuse extragalactic background radiation (DEBRA) [105] on sterile neutrinos decaying after recombination, i.e. $\tau > t_{\text{rec}}$ (the lower boundary of the DEBRA rejected region is indicated by a straight green line in Figs. 3 and (4)). X-ray limits coming from galaxies and galaxy clusters only apply to relatively recent times after these structures formed, thus they are superseded by the DEBRA limits which apply on the integrated flux of all decays that occur between t_{rec} and the present.

The 3.5 keV X-ray emission line signal reported in 2014 [47, 48], which remains a matter of lively debate (see e.g. [120, 121]), could be due to the decay of $m_s \simeq 7$ keV sterile neutrinos whose mixing should be $\sin^2 2\theta = 5 \times 10^{-11}$ if they constitute all of DM. The active-sterile mixing necessary for sterile neutrinos produced non-resonantly to reproduce the putative signal line shifts in the same way as the X-ray bounds just mentioned, and is indicated with a black star in Figs. (3) and (4). These figures show that in all the models we consider, except ST2, the signal would correspond to sterile neutrinos that constitute only a small

¹⁰The branching ratio for the photon decay channel is subdominant, the dominant decay channel is $\nu_s \rightarrow 3\nu_\alpha$.

fraction of the DM. Fig. 3 shows that in the ST2 model, the signal rejected by Lyman- α limits. Comparing the K, ST1 and LRT to the standard cosmology in Figs. 3 and (4), we see clearly that decreased production in cosmologies with faster expansion rates increases the mixing angle required to produce the signal. In the K cosmology the mixings necessary to produce the 3.5 keV signal is $\sin^2 2\theta = \mathcal{O}(10^{-9})$, and in the LRT and ST1 cosmologies it is $\sin^2 2\theta = \mathcal{O}(10^{-7})$, within the reach of the KATRIN experiment with its proposed TRISTAN upgrade [49] as well as the upcoming HUNTER experiment and its upgrades [50].

4.6.0 Laboratory experiments

For eV- and keV-mass sterile neutrinos, multiple laboratory experiments can probe and restrict sizable portions of the parameter space. Since these experiments directly probe the active-sterile mixing angle and mass by searching for active neutrino appearance and disappearance, the resulting bounds they set are independent of cosmology and require no further modification.

In the eV-mass range of sterile neutrinos mixing with ν_e , the limits are dominated by the Daya Bay [39], Bugey-3 [40] and PROSPECT [41] reactor and accelerator experiments, which combined reject the green regions labelled “R” in Figs. 3 and (4). Several anomalous results, consistent with a sterile neutrino of $m_s \sim$ eV mass contributing to active-sterile neutrino oscillations, have been reported from the short-baseline studies of ν_e appearance by the LSND [25] and MiniBooNE [26] experiments. These claims have been further bolstered recently with analysis of additional MiniBooNE data [27]. We show in Figs. 3 and (4) with a black densely hatched band denoted “MB” the parameter space allowed at the 4- σ level consistent with these excesses, reproduced from Fig. 4 of Ref. [27] (see discussions in Ref. [27] for details). We stress, however, that the anomalous ν_e appearance results discussed above are in strong tension with the ν_μ disappearance results from IceCube [122] and MINOS [123]. In the same sterile neutrino mass region, recent reactor neutrino results from the DANSS [37] and NEOS [38] experiments are also consistent with a sterile neutrino interpretation. A combined fit to their data [34–36] allows for a sterile neutrino with $m_s \simeq 1.14$ eV mass and $\sin^2 2\theta \simeq 0.04$ mixing with a ν_e active neutrino. The regions allowed at 3- σ level by the DANSS and NEOS data reproduced from Fig. 4 of Ref. [35] are indicated with black vertical elliptical contours in Figs. 3 and 4.

As we display in Fig. 3 and (4), the eV-mass parameter space relevant for anomalous observations in short-baseline and reactor experiments will be fully or at least partially tested by KATRIN [43] (whose reach is shown with a solid blue line labeled “KA”) as well as PTOLEMY [42] (whose reach is shown with solid orange lines labeled “P” and “P2” for 10 mg-yr and 100 g-yr exposures, respectively). PTOLEMY is a tritium β -decay experiment aimed at detecting the cosmological relic neutrino background which is expected to start collecting data within few years. As shown in Fig. 3 and Fig. 4, the cosmological bounds in the ST1 and LRT cosmologies are significantly relaxed for eV-mass sterile neutrinos compared to those in the Std cosmology. Hence, the required parameter space for anomalous observations

in short-baseline and reactor experiments is not rejected by cosmology.

In the keV mass-scale, the tritium decay experiment KATRIN [124, 125] will probe active-sterile mixing down to $\sin^2(2\theta) \leq 10^{-4}$ [49], shown with solid blue and denoted “KA” on Figs. 3 and 4. Its upgraded version, TRISTAN (denoted with a solid blue line and labelled “T” and “T2”, corresponding to a 1 year and 3 year data collecting period, respectively), is expected to reach sensitivities of $\sin^2(2\theta) \sim 10^{-8}$ within a 3 year run-time [49]. The upcoming cesium trap experiment HUNTER [50] is expected to probe even more further within the sterile neutrino parameter space. Here, the missing mass of the neutrino will be reconstructed from ^{131}Cs electron capture decays occurring in a magneto-optically trapped sample. The prototype version of the experiment is already under construction and will have two phases, whose sensitivity we display in Figs. 3 and (4) with magenta solid lines and labelled “H1A” and “H1B”, respectively. The upgrade version of Hunter, denoted by “HU”, is expected to be sensitive to mixings down to $\sin^2(2\theta) \sim 10^{-11}$. The above-mentioned experiments will be able to test the sterile neutrino origin of the 3.5 keV X-ray signal line. In non-standard cosmologies that result in decreased sterile neutrino density, the required mixing angle to explain the signal increases, allowing for sterile neutrinos to appear more visible for laboratory studies (see e.g. LRT and ST1 in Figs. 3 and (4)).

If the sterile neutrinos are Majorana particles, they will mediate the neutrinoless double beta $0\nu\beta\beta$ decay. A sterile neutrino that mixes with the electron neutrino contributes $\langle m \rangle_s = m_s \sin^2(\theta) e^{i\beta_s}$ to the effective electron neutrino Majorana mass $\langle m \rangle$ that affects the half-life of $0\nu\beta\beta$ decay, where β_s denotes a Majorana CP-violating phase. Hence, using the present bound on the magnitude of $\langle m \rangle$, $|\langle m \rangle| < 0.165$ eV [106], the corresponding bound on the sterile neutrino mass and mixing angle is $m_s \sin^2(2\theta) < 0.660$ eV. This limit is shown in orange in Figs. 3 and (4), with the label “ $0\nu\beta\beta$ ”. We note that this bound is not completely robust. The contribution of the sterile neutrino might interfere with the contributions from the active ones, leading to a suppression in the effective Majorana mass and, therefore, avoiding the experimental bounds [126].

5 Summary

The early Universe pre-BBN cosmology could be drastically different from the usually assumed radiation-dominated cosmology with SM particle content, as happens in motivated theoretical models – for example in models based on moduli or quintessence. Since no remnant has been detected from the pre-BBN epoch, this era of the early Universe currently remains completely untested. Visible sterile neutrinos, those which could be detected in near future laboratory experiments, could be the first remnants from this epoch. Here we revisited the production of sterile neutrinos via non-resonant active-sterile oscillations assuming different cosmologies before the temperature of the Universe was 5 MeV and showed that these neutrinos can act as sensitive probes of the pre-BBN cosmology.

In particular, we studied non-resonant sterile neutrino production within the standard and several non-standard cosmologies before $T = 5$ MeV. We dealt mostly with cosmological

models in which entropy in matter and radiation is conserved, such as the Scalar Tensor and Kination models, using a parameterization of the expansion rate H in terms of its amplitude and temperature dependence that has the particular cosmologies we studied as special cases. We also revisited Low Reheating Temperatures models, in which entropy is not conserved during the non-standard cosmological phase, but sterile neutrinos are produced dominantly in the standard phase, at $T < 5$ MeV. In all cases we assumed that the cosmology is standard at $T < 5$ MeV.

We found that the resulting sterile neutrino relic abundance can be either suppressed or enhanced and that the momentum distribution can be colder or hotter compared to those in the standard cosmology for the same neutrino masses and mixings. We derived general expressions for all relevant quantities using the mentioned parametrization of H with two parameters, and give them also for the particular cosmological models we studied. We updated and extended the cosmological and astrophysical bounds on all the cosmologies we considered.

In particular, in the Low Reheating Temperature and one of the Scalar Tensor (ST1) models we studied, the cosmological bounds are significantly relaxed, and the mixing of the sterile neutrinos possibly responsible for the 3.5 keV signal is more accessible to the reach of the upcoming KATRIN/TRISTAN and HUNTER experiments. These experiments have already started or are expected to start taking data soon. The observation of a ~ 7 keV mass sterile neutrino in one of them would not only constitute a momentous discovery in particle physics, but also in cosmology, even if this neutrino does not constitute all of the dark matter. Namely, it would not only constitute the discovery of a new elementary particle, a particle physics discovery of fundamental importance, but could hold vital information about the pre-BBN cosmology from which this sterile neutrino could be the first ever detected remnant.

For example, if the measured mixing would be $\sin^2 2\theta = \mathcal{O}(10^{-7})$, the discovery would be consistent with a non-standard cosmology such as the ST1 and Low Reheating Temperature we studied here. On the other hand, a measured value of $\sin^2 2\theta = \mathcal{O}(10^{-9})$ could instead point towards a Kination model (or maybe special particle models, e.g. [127]). For a $\sin^2 2\theta = \mathcal{O}(10^{-10})$, it would point to a standard pre-BBN cosmology, as indicated in Figs. 3 and (4) (see the location of the black stars).

The relaxation of cosmological bounds on eV-scale mass sterile neutrinos in non-standard pre-BBN cosmologies, mostly in the Low Reheating Temperature and the ST1 models, allows for the results reported from the LSND, and MiniBooNE short-baseline as well as the DANSS and NEOS reactor neutrino experiments to be unrestricted by cosmology¹¹. If the discovery of a sterile neutrino in any of these experiments would be confirmed, again this would be of fundamental importance not only for particle physics, but possibly for the pre-BBN cosmology in which they were produced, and it could provide an indication of a non-standard cosmology in this yet untested epoch.

¹¹The cosmological limits can be also suppressed by additional sterile neutrino interactions, such as those due to their coupling to an ultra-light scalar (see e.g. Refs. [128, 129]).

Acknowledgments

The work of G.B.G., P.L. and V.T. was supported in part by the U.S. Department of Energy (DOE) Grant No. DE-SC0009937.

A Additional formulas for non-resonant production

Below we show the equations in their general form as function of the η and β parameters appearing in the parametrization of H given in Eq. (2.2) and for the K, ST2 and LRT cosmologies, which were not given in the main text.

We give the equations for the following quantities: the temperature of maximum rate of production T_{\max} (except for the LRT model in which the maximum rate of production is at T_{RH}), the sterile neutrino momentum distributions $f_{\nu_s}(\epsilon)$ as function of the diensional momentum $\epsilon = p/T$, the relic number density n_{ν_s} and the relic energy density ρ_{ν_s} in general and at present, the present fraction $f_{s,\text{DM}}$ of the DM consisting of sterile neutrinos, and the mixing and function of mass $\sin^2(2\theta)_{\text{DW,lim}}$ for which this fraction is 1.

In the main text we included only the Std and the ST1 to easily compare the standard cosmology with the alternative cosmology that provides the largest departure from the standard results.

A.1.0 Temperature of maximum rate of production of sterile neutrinos

For the parametrization of H in Eq. (2.2) the temperature of maximum DW production for $\beta \leq 2$ is

$$T_{\max} \simeq 190 \text{ MeV } \epsilon^{-\frac{1}{3}} \left(\frac{2 - \beta}{10 + \beta} \right)^{\frac{1}{6}} \left(\frac{m_s}{\text{keV}} \right)^{\frac{1}{3}} \left(\frac{B}{10.88 \times 10^{-9} \text{ GeV}^{-4}} \right)^{-\frac{1}{6}}. \quad (\text{A.1})$$

In K pre-BBN cosmology ($\beta = 1$) it is

$$T_{\max}^{\text{K}} = 127 \text{ MeV } \epsilon^{-\frac{1}{3}} \left(\frac{m_s}{\text{keV}} \right)^{\frac{1}{3}} \left(\frac{B}{10.88 \times 10^{-9} \text{ GeV}^{-4}} \right)^{-\frac{1}{6}}, \quad (\text{A.2})$$

and the ST2 cosmology ($\beta = 0$),

$$T_{\max}^{\text{ST2}} = T_{\max}^{\text{Std}} = 145 \text{ MeV } \epsilon^{-\frac{1}{3}} \left(\frac{m_s}{\text{keV}} \right)^{\frac{1}{3}} \left(\frac{B}{10.88 \times 10^{-9} \text{ GeV}^{-4}} \right)^{-\frac{1}{6}}. \quad (\text{A.3})$$

The T_{\max} for ST2 and the standard cosmology coincide, because $\beta = 0$ for both.

A.2.0 Momentum distribution functions of non-resonantly produced sterile neutrinos

For the parametrization of H in Eq. (2.2) the momentum distribution function, as function of $\epsilon = p/T$, is given by

$$\begin{aligned}
 f_{\nu_s}(\epsilon) &= 3.08 \times 10^{-6} \eta^{-1} \epsilon^{\frac{\beta}{3}} (3 + \beta) (2.63 \times 10^{-2})^\beta \sec\left(\frac{\beta\pi}{6}\right) \left(\frac{\sin^2(2\theta)}{10^{-10}}\right) \\
 &\times \left(\frac{m_s}{\text{keV}}\right)^{1-\frac{\beta}{3}} \left(\frac{T_{\text{tr}}}{5 \text{ MeV}}\right)^\beta \left(\frac{g_*}{30}\right)^{-\frac{1}{2}} \left(\frac{d_\alpha}{1.13}\right) \\
 &\times \left(\frac{B}{10.88 \times 10^{-9} \text{ GeV}^{-4}}\right)^{-\frac{1}{2}+\frac{\beta}{6}} f_{\nu_\alpha}(\epsilon) .
 \end{aligned} \tag{A.4}$$

In the K cosmology $\eta = 1$, $\beta = 1$, thus

$$\begin{aligned}
 f_{\nu_s}^{\text{K}}(\epsilon) &= 3.74 \times 10^{-7} \epsilon^{\frac{1}{3}} \left(\frac{\sin^2(2\theta)}{10^{-10}}\right) \left(\frac{m_s}{\text{keV}}\right)^{\frac{2}{3}} \left(\frac{T_{\text{tr}}}{5 \text{ MeV}}\right) \left(\frac{g_*}{30}\right)^{-\frac{1}{2}} \\
 &\times \left(\frac{d_\alpha}{1.13}\right) \left(\frac{B}{10.88 \times 10^{-9} \text{ GeV}^{-4}}\right)^{-\frac{1}{3}} f_{\nu_\alpha}(\epsilon)
 \end{aligned} \tag{A.5}$$

and in the ST2 cosmology, $\eta = 0.03$ and $\beta = 0$, instead

$$\begin{aligned}
 f_{\nu_s}^{\text{ST2}}(\epsilon) &= 2.89 \times 10^{-4} \left(\frac{\sin^2(2\theta)}{10^{-10}}\right) \left(\frac{m_s}{\text{keV}}\right) \left(\frac{g_*}{30}\right)^{-\frac{1}{2}} \\
 &\times \left(\frac{d_\alpha}{1.13}\right) \left(\frac{B}{10.88 \times 10^{-9} \text{ GeV}^{-4}}\right)^{-\frac{1}{2}} f_{\nu_\alpha}(\epsilon) .
 \end{aligned} \tag{A.6}$$

The distribution function of sterile neutrinos for low reheating temperature (LRT) cosmologies is given in Eq. (1) of Ref. [57], for $T_{\text{RH}} = T_{\text{tr}}$. In these models sterile neutrinos are dominantly produced during the radiation-dominated period, i.e. for $T < T_{\text{RH}}$. We reproduce it here for completeness,

$$f_{\nu_s}^{\text{LRT}} = 3.6 \times 10^{-10} \epsilon \left(\frac{\sin^2(2\theta)}{10^{-10}}\right) \left(\frac{T_{\text{tr}}}{5 \text{ MeV}}\right)^3 \left(\frac{d_\alpha}{1.13}\right) f_{\nu_\alpha}(\epsilon) . \tag{A.7}$$

For consistency of notation, here use T_{tr} for the reheating temperature.

A.3.0 Relic number density of non-resonantly produced sterile neutrinos

The ratio of the number density of non-resonantly produced sterile neutrinos and of active neutrinos at the same temperature T is easily related to the ratio of their momentum

distributions,

$$\frac{n_{\nu_s}(T)}{n_{\nu_\alpha}(T)} = \epsilon^{-\frac{\beta}{3}} \frac{F_{2+\frac{\beta}{3}}(0)}{F_2(0)} \frac{f_{\nu_s}(\epsilon)}{f_{\nu_\alpha}(\epsilon)}. \quad (\text{A.8})$$

where we have used the η and β parametrization of H and the number density of active neutrinos (and antineutrinos) here is $n_{\nu_\alpha} = (3\zeta(3)/2\pi^2) T^3$. For each cosmology, this ratio is

$$\frac{n_{\nu_s}(T)}{n_{\nu_\alpha}(T)} = \frac{f_{\nu_s}(\epsilon)}{f_{\nu_\alpha}(\epsilon)} \times \begin{cases} 1, & \text{Std, ST2} \\ 1.42 \epsilon^{-0.33}, & \text{K} \\ 0.77 \epsilon^{0.27}, & \text{ST1} \\ 3.15 \epsilon^{-1}, & \text{LRH} \end{cases} \quad (\text{A.9})$$

The present number density of non-resonantly produced sterile neutrinos as a function of the η and β parameters of H in Eq. (2.2) is

$$\begin{aligned} n_{\nu_s} &= 7.81 \times 10^{-3} \text{cm}^{-3} \eta^{-1} (2.63 \times 10^{-2})^\beta (1 - 2^{-2-\frac{\beta}{3}}) \zeta\left(3 + \frac{\beta}{3}\right) \Gamma\left(3 + \frac{\beta}{3}\right) \\ &\times \left(\frac{3 + \beta}{36\pi}\right) \sec\left(\frac{\beta\pi}{6}\right) \left(\frac{\sin^2(2\theta)}{10^{-10}}\right) \left(\frac{m_s}{\text{keV}}\right)^{1-\frac{\beta}{3}} \left(\frac{T_{\text{tr}}}{5 \text{ MeV}}\right)^\beta \left(\frac{T_{\nu,0}}{1.95 \text{ K}}\right)^3 \\ &\times \left(\frac{g_*}{30}\right)^{-\frac{3}{2}} \left(\frac{d_\alpha}{1.13}\right) \left(\frac{B}{10.88 \times 10^{-9} \text{ GeV}^{-4}}\right)^{-\frac{1}{2} + \frac{\beta}{6}}. \end{aligned} \quad (\text{A.10})$$

Here g_* is the number of relativistic degrees of freedom when sterile neutrinos are produced, which we take to be $g_*(T_{\text{max}})$ thus at present the ratio of temperatures of the sterile and active neutrinos is $(T_{\nu_s,0}/T_{\nu,0}) = (g_*/10.75)^{1/3}$. $T_{\nu,0} = 1.95 \text{ K}$ is the present temperature of the relic active neutrino bath.

For K ($\eta = 1, \beta = 1$) the sterile neutrino number density is

$$\begin{aligned} n_{\nu_s}^{\text{K}}(T_{\nu_s}) &= 5.29 \times 10^{-7} \left(\frac{\sin^2(2\theta)}{10^{-10}}\right) \left(\frac{m_s}{\text{keV}}\right)^{\frac{2}{3}} \left(\frac{T_{\text{tr}}}{5 \text{ MeV}}\right) \left(\frac{T_{\nu_s}}{T_{\nu_\alpha}}\right)^3 \left(\frac{g_*}{30}\right)^{-\frac{1}{2}} \\ &\times \left(\frac{d_\alpha}{1.13}\right) \left(\frac{B}{10.88 \times 10^{-9} \text{ GeV}^{-4}}\right)^{-\frac{1}{3}} n_{\nu_\alpha}(T_{\nu_\alpha}), \end{aligned} \quad (\text{A.11})$$

and the present number density is

$$\begin{aligned} n_{\nu_s}^{\text{K}} &= 2.14 \times 10^{-5} \text{cm}^{-3} \left(\frac{\sin^2(2\theta)}{10^{-10}}\right) \left(\frac{m_s}{\text{keV}}\right)^{\frac{2}{3}} \left(\frac{T_{\text{tr}}}{5 \text{ MeV}}\right) \left(\frac{T_{\nu,0}}{1.95 \text{ K}}\right)^3 \\ &\times \left(\frac{g_*}{30}\right)^{-\frac{3}{2}} \left(\frac{d_\alpha}{1.13}\right) \left(\frac{B}{10.88 \times 10^{-9} \text{ GeV}^{-4}}\right)^{-\frac{1}{3}}. \end{aligned} \quad (\text{A.12})$$

For ST2 ($\eta = 0.03$, $\beta = 0$) the number density is

$$n_{\nu_s}^{\text{ST2}}(T_{\nu_s}) = 2.89 \times 10^{-4} \left(\frac{\sin^2(2\theta)}{10^{-10}} \right) \left(\frac{m_s}{\text{keV}} \right) \left(\frac{T_{\nu_s}}{T_{\nu_\alpha}} \right)^3 \left(\frac{g_*}{30} \right)^{-\frac{1}{2}} \\ \times \left(\frac{d_\alpha}{1.13} \right) \left(\frac{B}{10.88 \times 10^{-9} \text{ GeV}^{-4}} \right)^{-\frac{1}{2}} n_{\nu_\alpha}(T_{\nu_\alpha}), \quad (\text{A.13})$$

and the present number density is

$$n_{\nu_s}^{\text{ST2}} = 1.17 \times 10^{-2} \text{ cm}^{-3} \left(\frac{\sin^2(2\theta)}{10^{-10}} \right) \left(\frac{m_s}{\text{keV}} \right) \left(\frac{T_{\nu,0}}{1.95 \text{ K}} \right)^3 \\ \times \left(\frac{g_*}{30} \right)^{-\frac{3}{2}} \left(\frac{d_\alpha}{1.13} \right) \left(\frac{B}{10.88 \times 10^{-9} \text{ GeV}^{-4}} \right)^{-\frac{1}{2}}. \quad (\text{A.14})$$

In the LRT cosmology (see Eq. 2 of Ref. [57]) the number density is

$$n_{\nu_s}^{\text{LRT}}(T_{\nu_s}) = 1.13 \times 10^{-9} \left(\frac{\sin^2(2\theta)}{10^{-10}} \right) \left(\frac{T_{\text{tr}}}{5 \text{ MeV}} \right)^3 \left(\frac{d_\alpha}{1.13} \right) n_{\nu_\alpha}(T_{\nu_\alpha}), \quad (\text{A.15})$$

and the present number density is

$$n_{\nu_s}^{\text{LRT}} = 1.28 \times 10^{-7} \text{ cm}^{-3} \left(\frac{\sin^2(2\theta)}{10^{-10}} \right) \left(\frac{T_{\text{tr}}}{5 \text{ MeV}} \right)^3 \left(\frac{T_{\nu,0}}{1.95 \text{ K}} \right)^3 \left(\frac{d_\alpha}{1.13} \right). \quad (\text{A.16})$$

A.4.0 Energy density of non-resonantly produced relativistic sterile neutrinos

The ratio of the energy density of non-resonantly produced relativistic sterile neutrinos and of relativistic active neutrinos at the same temperature T is easily related to their number density ratio, and momentum distribution ratios,

$$\frac{\rho_{\nu_s}(T)}{\rho_{\nu_\alpha}(T)} = \frac{F_{3+\frac{\beta}{3}}(0)}{F_3(0)} \frac{F_2(0)}{F_{2+\frac{\beta}{3}}(0)} \frac{n_{\nu_s}(T)}{n_{\nu_\alpha}(T)} = \epsilon^{-\frac{\beta}{3}} \frac{F_{3+\frac{\beta}{3}}(0)}{F_3(0)} \frac{f_{\nu_s}(\epsilon)}{f_{\nu_\alpha}(\epsilon)}. \quad (\text{A.17})$$

where the energy density of relativistic active neutrinos (and antineutrinos) is here $\rho_{\nu_\alpha} = (7\pi^2/120) T^4$. Hence,

$$\frac{\rho_{\nu_s}(T)}{\rho_{\nu_\alpha}(T)} = \frac{n_{\nu_s}(T)}{n_{\nu_\alpha}(T)} \times \begin{cases} 1, & \text{Std, ST2} \\ 1.10, & \text{K} \\ 0.92, & \text{ST1} \\ 1.30, & \text{LRH} \end{cases} \quad (\text{A.18})$$

The energy density of relativistic sterile neutrinos at temperature T_{ν_s} produced non resonantly when the number of degrees of freedom were g^* (we take this to be the g_* at

T_{max}), using the η and β parameterization of H , is

$$\begin{aligned} \rho_{\nu_s}(T_{\nu_s}) &= 4.40 \times 10^{26} \text{ MeV/cm}^3 \eta^{-1} (2.63 \times 10^{-2})^\beta (1 - 2^{-3-\frac{\beta}{3}}) \zeta\left(4 + \frac{\beta}{3}\right) \Gamma\left(4 + \frac{\beta}{3}\right) \\ &\times \left(\frac{3 + \beta}{36\pi}\right) \sec\left(\frac{\beta\pi}{6}\right) \left(\frac{\sin^2(2\theta)}{10^{-10}}\right) \left(\frac{m_s}{\text{keV}}\right)^{1-\frac{\beta}{3}} \left(\frac{T_{\text{tr}}}{5 \text{ MeV}}\right)^\beta \left(\frac{T_{\nu_s}}{\text{MeV}}\right)^4 \\ &\times \left(\frac{g_*}{30}\right)^{-\frac{11}{6}} \left(\frac{d_\alpha}{1.13}\right) \left(\frac{B}{10.88 \times 10^{-9} \text{ GeV}^{-4}}\right)^{-\frac{1}{2}+\frac{\beta}{6}}, \end{aligned} \quad (\text{A.19})$$

which for K becomes

$$\begin{aligned} \rho_{\nu_s}^{\text{K}}(T_{\nu_s}) &= 5.83 \times 10^{-7} \left(\frac{\sin^2(2\theta)}{10^{-10}}\right) \left(\frac{m_s}{\text{keV}}\right)^{\frac{2}{3}} \left(\frac{T_{\text{tr}}}{5 \text{ MeV}}\right) \left(\frac{T_{\nu_s}}{T_{\nu_\alpha}}\right)^4 \left(\frac{g_*}{30}\right)^{-\frac{1}{2}} \\ &\times \left(\frac{d_\alpha}{1.13}\right) \left(\frac{B}{10.88 \times 10^{-9} \text{ GeV}^{-4}}\right)^{-\frac{1}{3}} \rho_{\nu_\alpha}(T_{\nu_\alpha}), \end{aligned} \quad (\text{A.20})$$

or,

$$\begin{aligned} \rho_{\nu_s}^{\text{K}}(T_{\nu_s}) &= 4.37 \times 10^{25} \text{ MeV/cm}^3 \left(\frac{\sin^2(2\theta)}{10^{-10}}\right) \left(\frac{m_s}{\text{keV}}\right)^{\frac{2}{3}} \left(\frac{T_{\text{tr}}}{5 \text{ MeV}}\right) \left(\frac{T_{\nu_s}}{1 \text{ MeV}}\right)^4 \\ &\times \left(\frac{g_*}{30}\right)^{-\frac{1}{2}} \left(\frac{d_\alpha}{1.13}\right) \left(\frac{B}{10.88 \times 10^{-9} \text{ GeV}^{-4}}\right)^{-\frac{1}{3}}, \end{aligned} \quad (\text{A.21})$$

and for ST2 is

$$\begin{aligned} \rho_{\nu_s}^{\text{ST2}}(T_{\nu_s}) &= 2.89 \times 10^{-4} \left(\frac{\sin^2(2\theta)}{10^{-10}}\right) \left(\frac{m_s}{\text{keV}}\right) \left(\frac{T_{\nu_s}}{T_{\nu_\alpha}}\right)^4 \left(\frac{g_*}{30}\right)^{-(1/2)} \\ &\times \left(\frac{d_\alpha}{1.13}\right) \left(\frac{B}{10.88 \times 10^{-9} \text{ GeV}^{-4}}\right)^{-\frac{1}{2}} \rho_{\nu_\alpha}(T_{\nu_\alpha}), \end{aligned} \quad (\text{A.22})$$

or,

$$\begin{aligned} \rho_{\nu_s}^{\text{ST2}}(T_{\nu_s}) &= 2.17 \times 10^{28} \text{ MeV/cm}^3 \left(\frac{\sin^2(2\theta)}{10^{-10}}\right) \left(\frac{m_s}{\text{keV}}\right) \left(\frac{T_{\nu_s}}{1 \text{ MeV}}\right)^4 \\ &\times \left(\frac{g_*}{30}\right)^{-(1/2)} \left(\frac{d_\alpha}{1.13}\right) \left(\frac{B}{10.88 \times 10^{-9} \text{ GeV}^{-4}}\right)^{-\frac{1}{2}}. \end{aligned} \quad (\text{A.23})$$

In the LRT model, production happens only during the standard phase (i.e. when $\eta = 1$ and $\beta = 0$), at temperatures smaller than the reheating temperature T_{RH} , which we denote here T_{tr} , and is dominated by the production close to T_{tr} . For temperatures $m_s < T < T_{\text{tr}}$

the relic energy density in the LRT model is

$$\begin{aligned}\rho_{\nu_s}^{\text{LRT}}(T_{\nu_s}) &= 1.48 \times 10^{-9} \left(\frac{\sin^2(2\theta)}{10^{-10}} \right) \left(\frac{T_{\text{tr}}}{5 \text{ MeV}} \right)^3 \left(\frac{T_{\nu_s}}{T_{\nu_\alpha}} \right)^4 \left(\frac{d_\alpha}{1.13} \right) \rho_{\nu_\alpha}(T_{\nu_\alpha}) \\ &= 1.11 \times 10^{23} \text{ MeV/cm}^3 \left(\frac{\sin^2(2\theta)}{10^{-10}} \right) \left(\frac{T_{\text{tr}}}{5 \text{ MeV}} \right)^3 \left(\frac{T_{\nu_s}}{1 \text{ MeV}} \right)^4 \left(\frac{d_\alpha}{1.13} \right). \quad (\text{A.24})\end{aligned}$$

A.5.0 Present fraction of the DM in non-resonantly produced sterile neutrinos

The present fraction of DM comprised of non-relativistic sterile neutrinos at present as function of the η and β parameters in Eq. (2.2) is

$$\begin{aligned}f_{s,\text{DM}} &= \left(\frac{n_{\nu_s,0} m_s}{\rho_{\text{DM}}} \right) = \\ &= 4.59 \times 10^{-5} \eta^{-1} \left(2.63 \times 10^{-2} \right)^\beta (3 + \beta) \left(1 - 2^{-2-\frac{\beta}{3}} \right) \zeta \left(3 + \frac{\beta}{3} \right) \\ &\quad \times \Gamma \left(3 + \frac{\beta}{3} \right) \sec \left(\frac{\beta\pi}{6} \right) \left(\frac{\sin^2(2\theta)}{10^{-10}} \right) \left(\frac{m_s}{\text{keV}} \right)^{2-\frac{\beta}{3}} \left(\frac{T_{\text{tr}}}{5 \text{ MeV}} \right)^\beta \\ &\quad \times \left(\frac{T_{\nu,0}}{1.95 \text{ K}} \right)^3 \left(\frac{g_*}{30} \right)^{-\frac{3}{2}} \left(\frac{d_\alpha}{1.13} \right) \left(\frac{\Omega_{\text{DM}} h^2}{0.12} \right) \left(\frac{B}{10.88 \times 10^{-9} \text{ GeV}^{-4}} \right)^{-\frac{1}{2}+\frac{\beta}{6}}, \quad (\text{A.25})\end{aligned}$$

where $n_{\nu_s,0}$ is the present number density, g_* is the number of entropy degrees of freedom when the sterile neutrinos were produced, $g_* = g_*(T_{\text{max}})$, and $T_{\nu,0}$ is the present active neutrino temperature. Unless stated otherwise we take $g_* = 30$ for our figures. For the K cosmology ($\eta = 1, \beta = 1$) the fraction is

$$\begin{aligned}f_{s,\text{DM}}^{\text{K}} &= \left(\frac{n_{\nu_s,0} m_s}{\rho_{\text{DM}}} \right)^{\text{K}} = \\ &= 1.42 \times 10^{-5} \left(\frac{\sin^2(2\theta)}{10^{-10}} \right) \left(\frac{m_s}{\text{keV}} \right)^{\frac{5}{3}} \left(\frac{T_{\text{tr}}}{5 \text{ MeV}} \right) \left(\frac{T_{\nu,0}}{1.95 \text{ K}} \right)^3 \\ &\quad \times \left(\frac{g_*}{30} \right)^{-\frac{3}{2}} \left(\frac{d_\alpha}{1.13} \right) \left(\frac{\Omega_{\text{DM}} h^2}{0.12} \right) \left(\frac{B}{10.88 \times 10^{-9} \text{ GeV}^{-4}} \right)^{-\frac{1}{3}} \quad (\text{A.26})\end{aligned}$$

and for ST2 cosmology ($\eta = 0.03, \beta = 0$),

$$\begin{aligned}f_{s,\text{DM}}^{\text{ST2}} &= \left(\frac{n_{\nu_s,0} m_s}{\rho_{\text{DM}}} \right)^{\text{ST2}} = \\ &= 7.74 \times 10^{-3} \left(\frac{\sin^2(2\theta)}{10^{-10}} \right) \left(\frac{m_s}{\text{keV}} \right)^2 \left(\frac{T_{\nu,0}}{1.95 \text{ K}} \right)^3 \left(\frac{g_*}{30} \right)^{-\frac{3}{2}} \\ &\quad \times \left(\frac{d_\alpha}{1.13} \right) \left(\frac{\Omega_{\text{DM}} h^2}{0.12} \right) \left(\frac{B}{10.88 \times 10^{-9} \text{ GeV}^{-4}} \right)^{-\frac{1}{2}}. \quad (\text{A.27})\end{aligned}$$

In the LRT model with T_{tr} denoting the reheating temperature, the fraction is instead

$$\begin{aligned}
f_{s,\text{DM}}^{\text{LRT}} &= \left(\frac{n_{\nu_s,0} m_s}{\rho_{\text{DM}}} \right)^{\text{LRT}} = \\
&= 1 \times 10^{-7} \left(\frac{\sin^2(2\theta)}{10^{-10}} \right) \left(\frac{m_s}{\text{keV}} \right) \left(\frac{T_{\text{tr}}}{5\text{MeV}} \right)^3 \left(\frac{T_{\nu,0}}{1.95 \text{ K}} \right)^3 \\
&\quad \times \left(\frac{d_\alpha}{1.13} \right) \left(\frac{\Omega_{\text{DM}} h^2}{0.12} \right). \tag{A.28}
\end{aligned}$$

A.6.0 DM density limit

The limit on the sterile-active neutrino mixing angle from DM density, $f_{s,\text{DM}} \leq 1$ translates into $\sin^2(2\theta) < \sin^2(2\theta)_{\text{DW,lim}}$, as function of η and β in Eq. (2.2), where

$$\begin{aligned}
\sin^2(2\theta)_{\text{DW,lim}} &= 2.18 \times 10^{-6} \eta \left[\left(1 - 2^{-2-\frac{\beta}{3}} \right) \zeta \left(3 + \frac{\beta}{3} \right) \sec \left(\frac{\beta\pi}{6} \right) \Gamma \left(3 + \frac{\beta}{3} \right) (3 + \beta) \right]^{-1} \\
&\quad \times \left(2.63 \times 10^{-2} \right)^{-\beta} \left(\frac{m_s}{\text{keV}} \right)^{-2+\frac{\beta}{3}} \left(\frac{T_{\text{tr}}}{5 \text{ MeV}} \right)^{-\beta} \left(\frac{T_{\nu,0}}{1.95 \text{ K}} \right)^{-3} \left(\frac{g_*}{30} \right)^{\frac{3}{2}} \\
&\quad \times \left(\frac{d_\alpha}{1.13} \right)^{-1} \left(\frac{\Omega_{\text{DM}} h^2}{0.12} \right)^{-1} \left(\frac{B}{10.88 \times 10^{-9} \text{ GeV}^{-4}} \right)^{\frac{1}{2}-\frac{\beta}{6}}. \tag{A.29}
\end{aligned}$$

For the K model ($\eta = 1, \beta = 1$)

$$\begin{aligned}
\sin^2(2\theta)_{\text{DW,lim}}^{\text{K}} &= 7.03 \times 10^{-6} \left(\frac{m_s}{\text{keV}} \right)^{-\frac{5}{3}} \left(\frac{T_{\text{tr}}}{5 \text{ MeV}} \right)^{-1} \left(\frac{T_{\nu,0}}{1.95 \text{ K}} \right)^{-3} \left(\frac{g_*}{30} \right)^{\frac{3}{2}} \\
&\quad \times \left(\frac{d_\alpha}{1.13} \right)^{-1} \left(\frac{\Omega_{\text{DM}} h^2}{0.12} \right)^{-1} \left(\frac{B}{10.88 \times 10^{-9} \text{ GeV}^{-4}} \right)^{\frac{1}{3}}. \tag{A.30}
\end{aligned}$$

For ST2 ($\eta = 0.03, \beta = 0$) instead,

$$\begin{aligned}
\sin^2(2\theta)_{\text{DW,lim}}^{\text{ST2}} &= 1.29 \times 10^{-8} \left(\frac{m_s}{\text{keV}} \right)^{-2} \left(\frac{T_{\nu,0}}{1.95 \text{ K}} \right)^{-3} \left(\frac{g_*}{30} \right)^{\frac{3}{2}} \left(\frac{d_\alpha}{1.13} \right)^{-1} \\
&\quad \times \left(\frac{\Omega_{\text{DM}} h^2}{0.12} \right)^{-1} \left(\frac{B}{10.88 \times 10^{-9} \text{ GeV}^{-4}} \right)^{\frac{1}{2}}. \tag{A.31}
\end{aligned}$$

For the LRT model, with $T_{\text{tr}} = T_{\text{RH}}$,

$$\sin^2(2\theta)_{\text{DW,lim}}^{\text{LRT}} = 1 \times 10^{-3} \left(\frac{m_s}{\text{keV}} \right)^{-1} \left(\frac{T_{\text{tr}}}{5 \text{ MeV}} \right)^{-3} \left(\frac{T_{\nu,0}}{1.95 \text{ K}} \right)^{-3} \left(\frac{d_\alpha}{1.13} \right)^{-1} \left(\frac{\Omega_{\text{DM}} h^2}{0.12} \right)^{-1}. \tag{A.32}$$

References

- [1] P. F. de Salas, M. Lattanzi, G. Mangano, G. Miele, S. Pastor and O. Pisanti, *Bounds on very low reheating scenarios after Planck*, *Phys. Rev.* **D92** (2015) 123534 [[1511.00672](#)].
- [2] T. Hasegawa, N. Hiroshima, K. Kohri, R. S. L. Hansen, T. Tram and S. Hannestad, *MeV-scale reheating temperature and thermalization of oscillating neutrinos by radiative and hadronic decays of massive particles*, [1908.10189](#).
- [3] F. De Bernardis, L. Pagano and A. Melchiorri, *New constraints on the reheating temperature of the universe after WMAP-5*, *Astropart. Phys.* **30** (2008) 192.
- [4] S. Hannestad, *What is the lowest possible reheating temperature?*, *Phys. Rev.* **D70** (2004) 043506 [[astro-ph/0403291](#)].
- [5] M. Kawasaki, K. Kohri and N. Sugiyama, *MeV scale reheating temperature and thermalization of neutrino background*, *Phys. Rev.* **D62** (2000) 023506 [[astro-ph/0002127](#)].
- [6] M. Kawasaki, K. Kohri and N. Sugiyama, *Cosmological constraints on late time entropy production*, *Phys. Rev. Lett.* **82** (1999) 4168 [[astro-ph/9811437](#)].
- [7] ALEPH, DELPHI, L3, OPAL, SLD, LEP ELECTROWEAK WORKING GROUP, SLD ELECTROWEAK GROUP, SLD HEAVY FLAVOUR GROUP collaboration, S. Schael et al., *Precision electroweak measurements on the Z resonance*, *Phys. Rept.* **427** (2006) 257 [[hep-ex/0509008](#)].
- [8] SUPER-KAMIOKANDE collaboration, Y. Fukuda et al., *Evidence for oscillation of atmospheric neutrinos*, *Phys. Rev. Lett.* **81** (1998) 1562 [[hep-ex/9807003](#)].
- [9] B. T. Cleveland, T. Daily, R. Davis, Jr., J. R. Distel, K. Lande, C. K. Lee et al., *Measurement of the solar electron neutrino flux with the Homestake chlorine detector*, *Astrophys. J.* **496** (1998) 505.
- [10] SAGE collaboration, J. N. Abdurashitov et al., *Measurement of the solar neutrino capture rate with gallium metal. III: Results for the 2002–2007 data-taking period*, *Phys. Rev.* **C80** (2009) 015807 [[0901.2200](#)].
- [11] GNO collaboration, M. Altmann et al., *Complete results for five years of GNO solar neutrino observations*, *Phys. Lett.* **B616** (2005) 174 [[hep-ex/0504037](#)].
- [12] GALLEX collaboration, W. Hampel et al., *GALLEX solar neutrino observations: Results for GALLEX IV*, *Phys. Lett.* **B447** (1999) 127.
- [13] SNO collaboration, B. Aharmim et al., *Electron energy spectra, fluxes, and day-night asymmetries of B-8 solar neutrinos from measurements with NaCl dissolved in the heavy-water detector at the Sudbury Neutrino Observatory*, *Phys. Rev.* **C72** (2005) 055502 [[nucl-ex/0502021](#)].
- [14] SUPER-KAMIOKANDE collaboration, K. Abe et al., *Solar Neutrino Measurements in Super-Kamiokande-IV*, *Phys. Rev.* **D94** (2016) 052010 [[1606.07538](#)].
- [15] KAMLAND collaboration, T. Araki et al., *Measurement of neutrino oscillation with KamLAND: Evidence of spectral distortion*, *Phys. Rev. Lett.* **94** (2005) 081801 [[hep-ex/0406035](#)].

- [16] DAYA BAY collaboration, F. P. An et al., *Observation of electron-antineutrino disappearance at Daya Bay*, *Phys. Rev. Lett.* **108** (2012) 171803 [[1203.1669](#)].
- [17] DOUBLE CHOOZ collaboration, Y. Abe et al., *First Measurement of θ_{13} from Delayed Neutron Capture on Hydrogen in the Double Chooz Experiment*, *Phys. Lett.* **B723** (2013) 66 [[1301.2948](#)].
- [18] RENO collaboration, J. K. Ahn et al., *Observation of Reactor Electron Antineutrino Disappearance in the RENO Experiment*, *Phys. Rev. Lett.* **108** (2012) 191802 [[1204.0626](#)].
- [19] K2K collaboration, M. H. Ahn et al., *Measurement of Neutrino Oscillation by the K2K Experiment*, *Phys. Rev.* **D74** (2006) 072003 [[hep-ex/0606032](#)].
- [20] MINOS collaboration, P. Adamson et al., *Measurement of Neutrino and Antineutrino Oscillations Using Beam and Atmospheric Data in MINOS*, *Phys. Rev. Lett.* **110** (2013) 251801 [[1304.6335](#)].
- [21] T2K collaboration, K. Abe et al., *Precise Measurement of the Neutrino Mixing Parameter θ_{23} from Muon Neutrino Disappearance in an Off-Axis Beam*, *Phys. Rev. Lett.* **112** (2014) 181801 [[1403.1532](#)].
- [22] OPERA collaboration, N. Agafonova et al., *Evidence for $\nu_{\mu} \rightarrow \nu_{\tau}$ appearance in the CNGS neutrino beam with the OPERA experiment*, *Phys. Rev.* **D89** (2014) 051102 [[1401.2079](#)].
- [23] NOVA collaboration, P. Adamson et al., *First measurement of muon-neutrino disappearance in NOvA*, *Phys. Rev.* **D93** (2016) 051104 [[1601.05037](#)].
- [24] ICECUBE collaboration, M. G. Aartsen et al., *Determining neutrino oscillation parameters from atmospheric muon neutrino disappearance with three years of IceCube DeepCore data*, *Phys. Rev.* **D91** (2015) 072004 [[1410.7227](#)].
- [25] LSND collaboration, A. Aguilar-Arevalo et al., *Evidence for neutrino oscillations from the observation of anti-neutrino(electron) appearance in a anti-neutrino(muon) beam*, *Phys. Rev.* **D64** (2001) 112007 [[hep-ex/0104049](#)].
- [26] MINIBOONE collaboration, A. A. Aguilar-Arevalo et al., *Improved Search for $\bar{\nu}_{\mu} \rightarrow \bar{\nu}_e$ Oscillations in the MiniBooNE Experiment*, *Phys. Rev. Lett.* **110** (2013) 161801 [[1303.2588](#)].
- [27] MINIBOONE collaboration, A. A. Aguilar-Arevalo et al., *Significant Excess of ElectronLike Events in the MiniBooNE Short-Baseline Neutrino Experiment*, *Phys. Rev. Lett.* **121** (2018) 221801 [[1805.12028](#)].
- [28] J. Kostensalo, J. Suhonen, C. Giunti and P. C. Srivastava, *The gallium anomaly revisited*, *Phys. Lett.* **B795** (2019) 542 [[1906.10980](#)].
- [29] J. N. Bahcall, P. I. Krastev and E. Lisi, *Limits on electron-neutrino oscillations from the GALLEX Cr-51 source experiment*, *Phys. Lett.* **B348** (1995) 121 [[hep-ph/9411414](#)].
- [30] J. N. Abdurashitov et al., *Measurement of the response of a Ga solar neutrino experiment to neutrinos from an Ar-37 source*, *Phys. Rev.* **C73** (2006) 045805 [[nucl-ex/0512041](#)].
- [31] DAYA BAY collaboration, F. P. An et al., *Evolution of the Reactor Antineutrino Flux and Spectrum at Daya Bay*, *Phys. Rev. Lett.* **118** (2017) 251801 [[1704.01082](#)].
- [32] P. Huber, *NEOS Data and the Origin of the 5 MeV Bump in the Reactor Antineutrino Spectrum*, *Phys. Rev. Lett.* **118** (2017) 042502 [[1609.03910](#)].

- [33] G. Mention, M. Fechner, T. Lasserre, T. A. Mueller, D. Lhuillier, M. Cribier et al., *The Reactor Antineutrino Anomaly*, *Phys. Rev.* **D83** (2011) 073006 [[1101.2755](#)].
- [34] M. Dentler, A. Hernandez-Cabezudo, J. Kopp, P. A. N. Machado, M. Maltoni, I. Martinez-Soler et al., *Updated Global Analysis of Neutrino Oscillations in the Presence of eV-Scale Sterile Neutrinos*, *JHEP* **08** (2018) 010 [[1803.10661](#)].
- [35] S. Gariazzo, C. Giunti, M. Laveder and Y. F. Li, *Model-independent $\bar{\nu}_e$ short-baseline oscillations from reactor spectral ratios*, *Phys. Lett.* **B782** (2018) 13 [[1801.06467](#)].
- [36] J. Liao, D. Marfatia and K. Whisnant, *MiniBooNE, MINOS+ and IceCube data imply a baroque neutrino sector*, *Phys. Rev.* **D99** (2019) 015016 [[1810.01000](#)].
- [37] DANSS collaboration, I. Alekseev et al., *Search for sterile neutrinos at the DANSS experiment*, *Phys. Lett.* **B787** (2018) 56 [[1804.04046](#)].
- [38] NEOS collaboration, Y. J. Ko et al., *Sterile Neutrino Search at the NEOS Experiment*, *Phys. Rev. Lett.* **118** (2017) 121802 [[1610.05134](#)].
- [39] DAYA BAY collaboration, F. P. An et al., *Improved Search for a Light Sterile Neutrino with the Full Configuration of the Daya Bay Experiment*, *Phys. Rev. Lett.* **117** (2016) 151802 [[1607.01174](#)].
- [40] Y. Declais et al., *Search for neutrino oscillations at 15-meters, 40-meters, and 95-meters from a nuclear power reactor at Bugey*, *Nucl. Phys.* **B434** (1995) 503.
- [41] PROSPECT collaboration, J. Ashenfelter et al., *First search for short-baseline neutrino oscillations at HFIR with PROSPECT*, *Phys. Rev. Lett.* **121** (2018) 251802 [[1806.02784](#)].
- [42] PTOLEMY collaboration, M. G. Betti et al., *Neutrino physics with the PTOLEMY project: active neutrino properties and the light sterile case*, *JCAP* **1907** (2019) 047 [[1902.05508](#)].
- [43] KATRIN collaboration, F. Megas, *eV-scale Sterile Neutrino Investigation with the First Tritium KATRIN Data, Master's Thesis* .
- [44] A. Boyarsky, M. Drewes, T. Lasserre, S. Mertens and O. Ruchayskiy, *Sterile Neutrino Dark Matter*, *Prog. Part. Nucl. Phys.* **104** (2019) 1 [[1807.07938](#)].
- [45] A. Boyarsky, O. Ruchayskiy and D. Iakubovskiy, *A Lower bound on the mass of Dark Matter particles*, *JCAP* **0903** (2009) 005 [[0808.3902](#)].
- [46] A. Palazzo, D. Cumberbatch, A. Slosar and J. Silk, *Sterile neutrinos as subdominant warm dark matter*, *Phys. Rev.* **D76** (2007) 103511 [[0707.1495](#)].
- [47] E. Bulbul, M. Markevitch, A. Foster, R. K. Smith, M. Loewenstein and S. W. Randall, *Detection of An Unidentified Emission Line in the Stacked X-ray spectrum of Galaxy Clusters*, *Astrophys. J.* **789** (2014) 13 [[1402.2301](#)].
- [48] A. Boyarsky, O. Ruchayskiy, D. Iakubovskiy and J. Franse, *Unidentified Line in X-Ray Spectra of the Andromeda Galaxy and Perseus Galaxy Cluster*, *Phys. Rev. Lett.* **113** (2014) 251301 [[1402.4119](#)].
- [49] KATRIN collaboration, S. Mertens et al., *A novel detector system for KATRIN to search for keV-scale sterile neutrinos*, *J. Phys.* **G46** (2019) 065203 [[1810.06711](#)].

- [50] P. F. Smith, *Proposed experiments to detect keV range sterile neutrinos using energy-momentum reconstruction of beta decay or K-capture events*, *New J. Phys.* **21** (2019) 053022 [[1607.06876](#)].
- [51] G. M. Fuller, A. Kusenko, I. Mocioiu and S. Pascoli, *Pulsar kicks from a dark-matter sterile neutrino*, *Phys. Rev.* **D68** (2003) 103002 [[astro-ph/0307267](#)].
- [52] S. Dodelson and L. M. Widrow, *Sterile-neutrinos as dark matter*, *Phys. Rev. Lett.* **72** (1994) 17 [[hep-ph/9303287](#)].
- [53] X.-D. Shi and G. M. Fuller, *A New dark matter candidate: Nonthermal sterile neutrinos*, *Phys. Rev. Lett.* **82** (1999) 2832 [[astro-ph/9810076](#)].
- [54] K. Abazajian, G. M. Fuller and M. Patel, *Sterile neutrino hot, warm, and cold dark matter*, *Phys. Rev.* **D64** (2001) 023501 [[astro-ph/0101524](#)].
- [55] K. Abazajian, N. F. Bell, G. M. Fuller and Y. Y. Y. Wong, *Cosmological lepton asymmetry, primordial nucleosynthesis, and sterile neutrinos*, *Phys. Rev.* **D72** (2005) 063004 [[astro-ph/0410175](#)].
- [56] K. Petraki and A. Kusenko, *Dark-matter sterile neutrinos in models with a gauge singlet in the Higgs sector*, *Phys. Rev.* **D77** (2008) 065014 [[0711.4646](#)].
- [57] G. Gelmini, S. Palomares-Ruiz and S. Pascoli, *Low reheating temperature and the visible sterile neutrino*, *Phys. Rev. Lett.* **93** (2004) 081302 [[astro-ph/0403323](#)].
- [58] T. Rehagen and G. B. Gelmini, *Effects of kination and scalar-tensor cosmologies on sterile neutrinos*, *JCAP* **1406** (2014) 044 [[1402.0607](#)].
- [59] K. N. Abazajian, *Sterile neutrinos in cosmology*, *Phys. Rept.* **711-712** (2017) 1 [[1705.01837](#)].
- [60] G. B. Gelmini, P. Lu and V. Takhistov, *Visible Sterile Neutrinos as the Earliest Relic Probes of Cosmology*, [1909.04168](#).
- [61] E. W. Kolb and M. S. Turner, *The Early Universe*, *Front. Phys.* **69** (1990) 1.
- [62] L. Husdal, *On Effective Degrees of Freedom in the Early Universe*, *Galaxies* **4** (2016) 78 [[1609.04979](#)].
- [63] S. Borsanyi et al., *Calculation of the axion mass based on high-temperature lattice quantum chromodynamics*, *Nature* **539** (2016) 69 [[1606.07494](#)].
- [64] M. Drees, F. Hajkarim and E. R. Schmitz, *The Effects of QCD Equation of State on the Relic Density of WIMP Dark Matter*, *JCAP* **1506** (2015) 025 [[1503.03513](#)].
- [65] R. Catena, N. Fornengo, M. Pato, L. Pieri and A. Masiero, *Thermal Relics in Modified Cosmologies: Bounds on Evolution Histories of the Early Universe and Cosmological Boosts for PAMELA*, *Phys. Rev.* **D81** (2010) 123522 [[0912.4421](#)].
- [66] G. Gelmini and P. Gondolo, *DM Production Mechanisms*, [1009.3690](#).
- [67] M. Kamionkowski and M. S. Turner, *THERMAL RELICS: DO WE KNOW THEIR ABUNDANCES?*, *Phys. Rev.* **D42** (1990) 3310.
- [68] P. Salati, *Quintessence and the relic density of neutralinos*, *Phys. Lett.* **B571** (2003) 121 [[astro-ph/0207396](#)].

- [69] G. Lambiase, S. Mohanty and A. Stabile, *PeV IceCube signals and Dark Matter relic abundance in modified cosmologies*, *Eur. Phys. J.* **C78** (2018) 350 [[1804.07369](#)].
- [70] F. D’Eramo, N. Fernandez and S. Profumo, *When the Universe Expands Too Fast: Relentless Dark Matter*, *JCAP* **1705** (2017) 012 [[1703.04793](#)].
- [71] J. Khoury, B. A. Ovrut, P. J. Steinhardt and N. Turok, *The Ekpyrotic universe: Colliding branes and the origin of the hot big bang*, *Phys. Rev.* **D64** (2001) 123522 [[hep-th/0103239](#)].
- [72] L. Randall and R. Sundrum, *An Alternative to compactification*, *Phys. Rev. Lett.* **83** (1999) 4690 [[hep-th/9906064](#)].
- [73] M. Schelke, R. Catena, N. Fornengo, A. Masiero and M. Pietroni, *Constraining pre Big-Bang-Nucleosynthesis Expansion using Cosmic Antiprotons*, *Phys. Rev.* **D74** (2006) 083505 [[hep-ph/0605287](#)].
- [74] B. Spokoiny, *Deflationary universe scenario*, *Phys. Lett.* **B315** (1993) 40 [[gr-qc/9306008](#)].
- [75] M. Joyce, *Electroweak Baryogenesis and the Expansion Rate of the Universe*, *Phys. Rev.* **D55** (1997) 1875 [[hep-ph/9606223](#)].
- [76] S. Profumo and P. Ullio, *SUSY dark matter and quintessence*, *JCAP* **0311** (2003) 006 [[hep-ph/0309220](#)].
- [77] C. Pallis, *Quintessential kination and cold dark matter abundance*, *JCAP* **0510** (2005) 015 [[hep-ph/0503080](#)].
- [78] R. Catena, N. Fornengo, A. Masiero, M. Pietroni and F. Rosati, *Dark matter relic abundance and scalar - tensor dark energy*, *Phys. Rev.* **D70** (2004) 063519 [[astro-ph/0403614](#)].
- [79] A. A. Starobinsky, *A New Type of Isotropic Cosmological Models Without Singularity*, *Phys. Lett.* **B91** (1980) 99.
- [80] S. Capozziello, V. Galluzzi, G. Lambiase and L. Pizza, *Cosmological evolution of thermal relic particles in $f(R)$ gravity*, *Phys. Rev.* **D92** (2015) 084006 [[1507.06835](#)].
- [81] D. I. Santiago, D. Kalligas and R. V. Wagoner, *Scalar - tensor cosmologies and their late time evolution*, *Phys. Rev.* **D58** (1998) 124005 [[gr-qc/9805044](#)].
- [82] T. Koivisto, D. Wills and I. Zavala, *Dark D-brane Cosmology*, *JCAP* **1406** (2014) 036 [[1312.2597](#)].
- [83] R. Catena, N. Fornengo, A. Masiero, M. Pietroni and M. Schelke, *Enlarging $mSUGRA$ parameter space by decreasing pre-BBN Hubble rate in Scalar-Tensor Cosmologies*, *JHEP* **10** (2008) 003 [[0712.3173](#)].
- [84] J. Sakstein and B. Jain, *Implications of the Neutron Star Merger GW170817 for Cosmological Scalar-Tensor Theories*, *Phys. Rev. Lett.* **119** (2017) 251303 [[1710.05893](#)].
- [85] G. B. Gelmini and P. Gondolo, *Neutralino with the right cold dark matter abundance in (almost) any supersymmetric model*, *Phys. Rev.* **D74** (2006) 023510 [[hep-ph/0602230](#)].
- [86] G. Gelmini, P. Gondolo, A. Soldatenko and C. E. Yaguna, *The Effect of a late decaying scalar on the neutralino relic density*, *Phys. Rev.* **D74** (2006) 083514 [[hep-ph/0605016](#)].
- [87] T. Moroi, M. Yamaguchi and T. Yanagida, *On the solution to the Polonyi problem with 0 (10-TeV) gravitino mass in supergravity*, *Phys. Lett.* **B342** (1995) 105 [[hep-ph/9409367](#)].

- [88] M. Kawasaki, T. Moroi and T. Yanagida, *Constraint on the reheating temperature from the decay of the Polonyi field*, *Phys. Lett.* **B370** (1996) 52 [[hep-ph/9509399](#)].
- [89] T. Moroi and L. Randall, *Wino cold dark matter from anomaly mediated SUSY breaking*, *Nucl. Phys.* **B570** (2000) 455 [[hep-ph/9906527](#)].
- [90] M.-C. Chen and V. Takhistov, *Baryogenesis, Dark Matter, and Flavor Structure in Non-thermal Moduli Cosmology*, *JHEP* **05** (2019) 101 [[1812.09341](#)].
- [91] R. Kitano, H. Murayama and M. Ratz, *Unified origin of baryons and dark matter*, *Phys. Lett.* **B669** (2008) 145 [[0807.4313](#)].
- [92] M. Drees and F. Hajkarim, *Dark Matter Production in an Early Matter Dominated Era*, *JCAP* **1802** (2018) 057 [[1711.05007](#)].
- [93] M. Fujii and K. Hamaguchi, *Nonthermal dark matter via Affleck-Dine baryogenesis and its detection possibility*, *Phys. Rev.* **D66** (2002) 083501 [[hep-ph/0205044](#)].
- [94] C. E. Yaguna, *Sterile neutrino production in models with low reheating temperatures*, *JHEP* **06** (2007) 002 [[0706.0178](#)].
- [95] G. Gelmini, E. Osoba, S. Palomares-Ruiz and S. Pascoli, *MeV sterile neutrinos in low reheating temperature cosmological scenarios*, *JCAP* **0810** (2008) 029 [[0803.2735](#)].
- [96] A. D. Dolgov, *Neutrinos in cosmology*, *Phys. Rept.* **370** (2002) 333 [[hep-ph/0202122](#)].
- [97] R. Barbieri and A. Dolgov, *Bounds on Sterile-neutrinos from Nucleosynthesis*, *Phys. Lett.* **B237** (1990) 440.
- [98] K. Kainulainen, *Light Singlet Neutrinos and the Primordial Nucleosynthesis*, *Phys. Lett.* **B244** (1990) 191.
- [99] K. Kainulainen, J. Maalampi and J. T. Peltoniemi, *Inert neutrinos in supernovae*, *Nucl. Phys.* **B358** (1991) 435.
- [100] PARTICLE DATA GROUP collaboration, M. Tanabashi et al., *Review of Particle Physics*, *Phys. Rev.* **D98** (2018) 030001.
- [101] J. Baur, N. Palanque-Delabrouille, C. Yèche, A. Boyarsky, O. Ruchayskiy, E. Armengaud et al., *Constraints from Ly- α forests on non-thermal dark matter including resonantly-produced sterile neutrinos*, *JCAP* **1712** (2017) 013 [[1706.03118](#)].
- [102] K. C. Y. Ng, B. M. Roach, K. Perez, J. F. Beacom, S. Horiuchi, R. Krivonos et al., *New Constraints on Sterile Neutrino Dark Matter from NuSTAR M31 Observations*, *Phys. Rev.* **D99** (2019) 083005 [[1901.01262](#)].
- [103] K. Perez, K. C. Y. Ng, J. F. Beacom, C. Hersh, S. Horiuchi and R. Krivonos, *Almost closing the ν MSM sterile neutrino dark matter window with NuSTAR*, *Phys. Rev.* **D95** (2017) 123002 [[1609.00667](#)].
- [104] A. Neronov, D. Malyshev and D. Eckert, *Decaying dark matter search with NuSTAR deep sky observations*, *Phys. Rev.* **D94** (2016) 123504 [[1607.07328](#)].
- [105] A. Boyarsky, A. Neronov, O. Ruchayskiy and M. Shaposhnikov, *Constraints on sterile neutrino as a dark matter candidate from the diffuse x-ray background*, *Mon. Not. Roy. Astron. Soc.* **370** (2006) 213 [[astro-ph/0512509](#)].

- [106] KAMLAND-ZEN collaboration, A. Gando et al., *Search for Majorana Neutrinos near the Inverted Mass Hierarchy Region with KamLAND-Zen*, *Phys. Rev. Lett.* **117** (2016) 082503 [[1605.02889](#)].
- [107] D. J. Fixsen, E. S. Cheng, J. M. Gales, J. C. Mather, R. A. Shafer and E. L. Wright, *The Cosmic Microwave Background spectrum from the full COBE FIRAS data set*, *Astrophys. J.* **473** (1996) 576 [[astro-ph/9605054](#)].
- [108] M. Viel, J. Lesgourgues, M. G. Haehnelt, S. Matarrese and A. Riotto, *Constraining warm dark matter candidates including sterile neutrinos and light gravitinos with WMAP and the Lyman-alpha forest*, *Phys. Rev.* **D71** (2005) 063534 [[astro-ph/0501562](#)].
- [109] G. Mangano, G. Miele, S. Pastor, T. Pinto, O. Pisanti and P. D. Serpico, *Relic neutrino decoupling including flavor oscillations*, *Nucl. Phys.* **B729** (2005) 221 [[hep-ph/0506164](#)].
- [110] P. F. de Salas and S. Pastor, *Relic neutrino decoupling with flavour oscillations revisited*, *JCAP* **1607** (2016) 051 [[1606.06986](#)].
- [111] G. B. Gelmini, A. Kusenko and V. Takhistov, *Hints of Sterile Neutrinos in Recent Measurements of the Hubble Parameter*, [1906.10136](#).
- [112] PLANCK collaboration, N. Aghanim et al., *Planck 2018 results. VI. Cosmological parameters*, [1807.06209](#).
- [113] S. Roy Choudhury and S. Choubey, *Constraining light sterile neutrino mass with the BICEP2/Keck Array 2014 B-mode polarization data*, *Eur. Phys. J.* **C79** (2019) 557 [[1807.10294](#)].
- [114] J. R. Ellis, G. B. Gelmini, J. L. Lopez, D. V. Nanopoulos and S. Sarkar, *Astrophysical constraints on massive unstable neutral relic particles*, *Nucl. Phys.* **B373** (1992) 399.
- [115] W. Hu and J. Silk, *Thermalization constraints and spectral distortions for massive unstable relic particles*, *Phys. Rev. Lett.* **70** (1993) 2661.
- [116] G. G. Raffelt and S. Zhou, *Supernova bound on keV-mass sterile neutrinos reexamined*, *Phys. Rev.* **D83** (2011) 093014 [[1102.5124](#)].
- [117] C. A. Argüelles, V. Brdar and J. Kopp, *Production of keV Sterile Neutrinos in Supernovae: New Constraints and Gamma Ray Observables*, *Phys. Rev.* **D99** (2019) 043012 [[1605.00654](#)].
- [118] R. Shrock, *Decay $L^0 \rightarrow \nu_l \gamma$ in gauge theories of weak and electromagnetic interactions*, *Phys. Rev.* **D9** (1974) 743.
- [119] P. B. Pal and L. Wolfenstein, *Radiative Decays of Massive Neutrinos*, *Phys. Rev.* **D25** (1982) 766.
- [120] C. Dessert, N. L. Rodd and B. R. Safdi, *Evidence against the decaying dark matter interpretation of the 3.5 keV line from blank sky observations*, [1812.06976](#).
- [121] A. Boyarsky, D. Iakubovskiy, O. Ruchayskiy and D. Savchenko, *Surface brightness profile of the 3.5 keV line in the Milky Way halo*, [1812.10488](#).
- [122] ICECUBE collaboration, M. G. Aartsen et al., *Searches for Sterile Neutrinos with the IceCube Detector*, *Phys. Rev. Lett.* **117** (2016) 071801 [[1605.01990](#)].
- [123] MINOS+ collaboration, P. Adamson et al., *Search for sterile neutrinos in MINOS and MINOS+ using a two-detector fit*, *Phys. Rev. Lett.* **122** (2019) 091803 [[1710.06488](#)].

- [124] KATRIN collaboration, J. Wolf, *The KATRIN Neutrino Mass Experiment*, *Nucl. Instrum. Meth.* **A623** (2010) 442 [[0810.3281](#)].
- [125] KATRIN collaboration, S. Mertens, *Status of the KATRIN Experiment and Prospects to Search for keV-mass Sterile Neutrinos in Tritium β -decay*, *Phys. Procedia* **61** (2015) 267.
- [126] A. Abada, A. Hernandez-Cabezudo and X. Marciano, *Beta and Neutrinoless Double Beta Decays with KeV Sterile Fermions*, *JHEP* **01** (2019) 041 [[1807.01331](#)].
- [127] F. Bezrukov, A. Chudaykin and D. Gorbunov, *Hiding an elephant: heavy sterile neutrino with large mixing angle does not contradict cosmology*, *JCAP* **1706** (2017) 051 [[1705.02184](#)].
- [128] Y. Farzan, *Ultra-light scalar saving the 3+1 neutrino scheme from the cosmological bounds*, *Phys. Lett.* **B797** (2019) 134911 [[1907.04271](#)].
- [129] J. M. Cline, *Viable secret neutrino interactions with ultralight dark matter*, [1908.02278](#).